Inorganic Chemistry
Article

*Inorg. Chem.* **2009**, *48*, 7891–7904 **7891**
DOI: 10.1021/ic900764e

# Experimental and Computational Studies of Binding of Dinitrogen, Nitriles, Azides, Diazoalkanes, Pyridine, and Pyrazines to $M(PR_3)_2(CO)_3$ (M = Mo, W; R = Me, $^i$Pr).†

**Patrick Achord,‡ Etsuko Fujita,‡ James T. Muckerman,*,‡ Brian Scott,*,§ George C. Fortman,∥ Manuel Temprado,∥ Xiaochen Cai,∥ Burjor Captain,*,∥ Derek Isrow,∥ John J. Weir,∥ James Eric McDonough,∥ and Carl D. Hoff*,∥**

‡*Chemistry Department, Brookhaven National Laboratory, Upton, New York 11973,* §*Chemistry Division, MS-J514, Los Alamos National Laboratory, Los Alamos, New Mexico 87545, and* ∥*Department of Chemistry, University of Miami, Coral Gables, Florida 33146*

Received April 21, 2009

The enthalpies of binding of a number of N-donor ligands to the complex $Mo(P^iPr_3)_2(CO)_3$ in toluene have been determined by solution calorimetry and equilibrium measurements. The measured binding enthalpies span a range of ~10 kcal mol$^{-1}$: $\Delta H_{binding} = -8.8 \pm 1.2$ ($N_2$−$Mo(P^iPr_3)_2(CO)_3$); $-10.3 \pm 0.8$ ($N_2$); $-11.2 \pm 0.4$ ($AdN_3$ (Ad = 1-adamantyl)); $-13.8 \pm 0.5$ ($N_2CHSiMe_3$); $-14.9 \pm 0.9$ (pyrazine=pz); $-14.8 \pm 0.6$ (2,6-$Me_2$pz); $-15.5 \pm 1.8$ ($Me_2NCN$); $-16.6 \pm 0.4$ ($CH_3CN$); $-17.0 \pm 0.4$ (pyridine); $-17.5 \pm 0.8$ ([4-$CH_3$pz][$PF_6$] (in tetrahydrofuran)); $-17.6 \pm 0.4$ ($C_6H_5CN$); $-18.6 \pm 1.8$ ($N_2CHC(=O)OEt$); and $-19.3 \pm 2.5$ kcal mol$^{-1}$ (pz)$Mo(P^iPr_3)_2(CO)_3$. The value for the isonitrile AdNC ($-29.0 \pm 0.3$) is 12.3 kcal mol$^{-1}$ more exothermic than that of the nitrile AdCN ($-16.7 \pm 0.6$ kcal mol$^{-1}$). The enthalpies of binding of a range of arene nitrile ligands were also studied, and remarkably, most nitrile complexes were clustered within a 1 kcal mol$^{-1}$ range despite dramatic color changes and variation of $\nu_{CN}$. Computed structural and spectroscopic parameters for the complexes $Mo(P^iPr_3)_2(CO)_3L$ are in good agreement with experimental data. Computed binding enthalpies for $Mo(P^iPr_3)_2(CO)_3L$ exhibit considerable scatter and are generally smaller compared to the experimental values, but relative agreement is reasonable. Computed enthalpies of binding using a larger basis set for $Mo(PMe_3)_2(CO)_3L$ show a better fit to experimental data than that for $Mo(P^iPr_3)_2(CO)_3L$ using a smaller basis set. Crystal structures of $Mo(P^iPr_3)_2(CO)_3$(AdCN), $W(P^iPr_3)_2(CO)_3(Me_2NCN)$, $W(P^iPr_3)_2(CO)_3$(2,6-$F_2C_6H_3CN$), $W(P^iPr_3)_2(CO)_3$(2,4,6-$Me_3C_6H_2CN$), $W(P^iPr_3)_2(CO)_3$(2,6-$Me_2$pz), $W(P^iPr_3)_2(CO)_3$(AdCN), $Mo(P^iPr_3)_2(CO)_3$(AdNC), and $W(P^iPr_3)_2(CO)_3$(AdNC) are reported.

## Introduction

The first compounds characterized to bind $H_2$ as a molecule,[1] $M(PR_3)_2(CO)_3$ (M = Cr, Mo, W; R = isopropyl ($^i$Pr), cyclohexyl (Cy)), were discovered nearly 30 years ago.[2] They are ideal for studying physical aspects of binding and oxidative addition at a sterically constrained, active metal center.[3] Previously we have reported[4] computational analysis of the thermochemistry of ligand binding to $W(PCy_3)_2(CO)_3$ for a wide range of ligands. This report focuses on the binding of N donor ligands to $Mo(P^iPr_3)_2(CO)_3$.

In comparison to N-donor ligands, the organometallic thermochemistry of P donor ligands has been more extensively investigated.[5] Phosphines play an important role in modifying metal catalyst reactivity, and an understanding of the factors controlling this important bond has emerged in terms of the steric and electronic parameters originally delineated by Tolman[6] in 1977. For organometallic complexes, the bond to N donor ligands is generally more labile, and there have been relatively few studies of N donor ligand binding in organometallic thermochemistry. Taube[7] and coworkers have investigated enthalpies of binding to $[Ru(NH_3)_5(H_2O)]^{2+}$ in aqueous solution for a range of N-donor ligands. Dinitrogen was found to be a stronger ligand than

† The authors dedicate this paper to Dr. Gregory J. Kubas, Los Alamos National Laboratory.

*To whom correspondence should be addressed. E-mail: c.hoff@miami.edu.

(1) Kubas. G. J. *Metal Dihydrogen and σ-Bond Complexes*; Kluwer Academic/Plenum Publishers: New York, 2001.
(2) Kubas, G. J. *J. Chem. Soc., Chem. Commun.* **1980**, 61.
(3) (a) McDonough, J. E.; Weir, J. J.; Sukcharoenphon, K.; Hoff, C. D.; Kryatova, O. P.; Rybak-Akimova, E. V.; Scott, B. L.; Kubas, G. J.; Mendiratta, A.; Cummins, C. C. *J. Am. Chem. Soc.* **2006**, *128*, 10295. (b) Lang, R. F.; Ju, T. D.; Kiss, G.; Hoff, C. D.; Bryan, J. C.; Kubas, G. J. *J. Am. Chem. Soc.* **1994**, *116*, 7917. (c) Torres, L.; Moreno, M.; Lluch, J. M. *J. Phys. Chem. A* **2001**, *105*, 4676. (d) Rattan, G; Khalsa, K.; Kubas, G. J.; Unkefer, C. J.; Van der Sluys, L. S.; Kubat-Martin, K. A. *J. Am. Chem. Soc.* **1990**, *112*, 3855. (e) Gonzalez, A. A.; Hoff, C. D. *Inorg. Chem.* **1989**, *28*, 4295. (f) Gonzalez, A. A.; Zhang, K.; Nolan, S. P.; de la Vega, R. L.; Mukerjee, S. L.; Hoff, C. D.; Kubas, G. J. *Organometallics* **1988**, *7*, 2429.
(4) Muckerman, J. T.; Fujita, E.; Hoff, C. D.; Kubas, G. J. *J. Phys. Chem. B* **2007**, *111*, 6815.
(5) Hoff, C. D. *Prog. Inorg. Chem.* **1992**, *40*, 503.
(6) Tolman, C. A. *Chem. Rev.* **1977**, *77*, 313.
(7) (a) Armor, J. N.; Taube, H. *J. Am. Chem. Soc.* **1970**, *92*, 6170. (b) Wishart, J. F.; Taube, H.; Breslauer, K. J.; Isied, S. S. *Inorg. Chem.* **1984**, *23*, 2997.


Published on Web 07/21/2009

acetonitrile by ≈ 1 kcal mol$^{-1}$. Computation of the gas-phase enthalpies of binding of nitriles to $Ag^+$ were recently shown[8] to span a range of over 30 kcal mol$^{-1}$ depending on the substituent X in N≡C—X. Experimental data for binding to $Al^+$ in the gas phase showed a much more modest dependence on R of only 4−5 kcal mol$^{-1}$.[9] Mass spectroscopic studies of binding of alkyl nitriles and benzonitrile to $Ni^+$ and $Co^+$ showed a linear correlation with the proton affinity of the nitrile; however, the range was small with benzonitrile being favored over acetonitrile by ≈2 kcal mol$^{-1}$.[10] Kovacs and co-workers have shown an opposite trend in binding enthalpies where acetonitrile is favored over benzonitrile by ≈2 kcal mol$^{-1}$ in $Fe^{III}$ complexes which are models for nitrile hydratase.[11]

This work reports on an experimental and computational investigation of bonding in the complexes $Mo(CO)_3(P^iPr_3)_2(NX)$ where NX can be N≡N, N≡CR, N≡N−NR, N=N=CHR, and other N-atom donors as a function of R to try to assess the role of $\pi$ bonding in these systems. There are reasons to anticipate that $\pi$ bonding may play an important, possibly dominant role. It is generally held that in terms of bonding ability to a metal complex, $N_2$ is intrinsically inferior to CO both as a $\sigma$ donor and a $\pi$ acceptor. Computations by Frenking[12] imply that $N_2$ binds mainly through metal→$N_2$ back-bonding. Similar conclusions have been made regarding binding to $[Mn(PCy_3)_2(CO)_3]^{+1}$: "$N_2$ is an exceedingly poor electron donor, even toward strong electrophiles, where it is much feebler than the weakest known ligands, e.g., $CH_2Cl_2$. The complete lack of binding to $[Mn(PCy_3)_2(CO)_3][B(C_6H_3(3,5\text{-}CF_3)_2)_4]$ and other electron-poor cationic complexes indicates that $N_2$ apparently can only be stabilized on a metal center by a high degree of $\pi$−back donation, even in actinide complexes."[13]

The importance of $\pi$-backbonding and electron delocalization in $Cr(CO)_5(CHX)$ (X = H, OH, $OCH_3$, $NH_2$, $NHCH_3$) complexes was highlighted by work of Frenking which showed that differences in the Cr=C bond in $Cr(CO)_5(CHX)$ depend mainly on the $\pi$-bonding ability of X and that the strong bond present when X = H (97.9 kcal mol$^{-1}$) is nearly 30 kcal mol$^{-1}$ weaker when X = $NH_2$ (68.7 kcal mol$^{-1}$).[14] Gusev has recently[15] computed donor properties for a range of two-electron donors and concluded that nitrogen donors follow the order $NMe_3$ > $NH_3$ > oxazoline > pyridine > MeN=$CH_2$ > acetonitrile ≫ $N_2$ with respect to $\sigma$ donating properties in metal complexes. The situation with respect to $\pi$-bonding for NX ligands is not clear except for the widespread belief that it is a dominant factor controlling $N_2$ binding to metals.

## Experimental Section

**General Considerations.** Unless stated otherwise, all operations were performed in a drybox under an atmosphere of purified argon. Toluene, tetrahydrofuran (THF), benzene, heptane, and octane were distilled over sodium metal before use. Distilled solvents were transferred under out-flow of argon into vacuum-tight vessels and were degassed before being transferred into the drybox. $C_6D_6$ was purchased from Sigma-Aldrich. Compounds $M(P^iPr_3)_2(CO)_3$ (M = W, Mo) were prepared;[16] AdNC was crystallized from a $CH_2Cl_2$/heptane mixture and sublimed at ≈ 85 °C before use.[17] All other compounds were used as received. $^1$H NMR spectra were recorded on a Bruker AVANCE-400 spectrometer at $T$ = 20 °C. Chemical shifts are reported with respect to internal solvent: 7.16 ppm ($C_6D_6$). FTIR spectra were obtained using a Perkin-Elmer 2000 FTIR/Microscope system that has been described elsewhere.[18] UV−vis spectra were recorded on a Perkin-Elmer Lambda 900 spectrophotometer.

**Synthesis of $Mo(P^iPr_3)_2(CO)_3$(L) (L = 2,6-$Me_2$pz (pz = pyrazine), $Me_2NCN$, 4-$Me_2NC_6H_4CN$, $C_6F_5CN$, $CH_3CN$, AdCN (Ad = 1-adamantyl), 2,4,6-$Me_3C_6H_2CN$, 2,6-$F_2C_6H_3CN$, $N_2CHSiMe_3$, $N_2CHC(=O)OEt$, $NC_5H_5$ (pyridine), 4-$CF_3C_6H_4CN$, [4-Mepz][$PF_6$], $C_6H_5CN$, AdNC.).** All syntheses were performed in a similar manner. In a representative preparation a 20 mL scintillation vial was charged with 0.20 mmol of $Mo(P^iPr_3)_2(CO)_3$ and an equimolar amount of AdNC. 5.0 mL of toluene were added. The reaction solution instantaneously turned from brown to yellow. The solvent was then removed under reduced pressure. The solid was then washed twice with a minimal amount of heptane to remove excess ligand and $M(P^iPr_3)_2(CO)_4$. A yield of 0.114 g (86% yield) of yellow crystalline $M(P^iPr_3)_2(CO)_3$(AdNC) was recovered. All products except the $N_2CHSiMe_3$ and $N_2CHC(=O)OEt$ complexes were recovered with spectroscopic yields of 100% and isolated yields of >75%. The complexes of $N_2CHSiMe_3$ and $N_2CHC(=O)OEt$ were formed quantitatively based on FTIR and NMR analysis; however, the initially formed complexes decomposed to unknown products upon removal of solvent and isolated yields could not be determined. FTIR spectral data for the $N_2CHSiMe_3$ and $N_2CHC(=O)OEt$ complexes are listed in the Supporting Information, Tables ST-2 and ST-3. $^1$H NMR shifts ($C_6D_6$) in ppm were: 2,6-$Me_2$pz, 1.23 36H(q), 2.12 6H(m), 8.76 2H (s), 2.00 6H(s); $Me_2NCN$, 1.39 36H(q), 2.36 6H(m), 1.79 6H(s); 4-$Me_2NC_6H_4CN$, 1.45 36H(q), 2.44 6H(m), 7.13 2H(d), 6.04 2H(d), 2.21 6H(s); $C_6F_5CN$, 1.39 36H(q), 2.41 6H(m); $CH_3CN$, 1.35 36H (q), 2.32 6H(m), 0.67 3H(s); AdCN, 1.40 36H(q), 2.40 6H(m), 1.59 6H(d), 1.50 3H(m), 1.24 6H(m); 2,4,6-$MeC_6H_2CN$, 1.38 36H(q), 2.39 6H(m), 6.36 2H(s), 2.28 6H(s), 1.83 3H(s); 2,6-$F_2C_6H_3CN$, 1.40 36H(q), 2.42 6H(m), 6.28 1H(m), 6.04 2H(t); $NC_5H_5$, 1.25 36H(q), 2.11 6H(m), 8.90 2H, 6.15 2H, 6.61 1H; 4-$CF_3C_6H_4$, 1.37 36H(q), 2.38 6H(m), 6.92 2H, 6.89 2H; $N_2CHSiMe_3$, 1.27 36H(q), 2.22 2.38 6H(m), 2.78 1H(s) 0.03 9H(s); $C_6H_5CN$, 1.38 36H(q), 2.38 6H(m), 7.04 2H(d), 6.84 2H(t), 6.74 1H(t); $N_2CHC(=O)OC_2H_5$, 1.23 36H(q), 2.24 6H(m); AdNC, 1.38 36H(q), 2.39 6H (m), 1.75 6H(d), 1.68 3H(m), 1.28 6H(m).

**Synthesis of $W(P^iPr_3)_2(CO)_3$(L) (L = 2,6-$Me_2$pz, $Me_2NCN$, AdCN, 2,4,6-$MeC_6H_2CN$, 2,6-$F_2C_6H_3CN$, AdNC.).** Syntheses were the same as the Mo analogues. All yields were >75%. $^1$H NMR shifts ($C_6D_6$) ppm: 2,6-$Me_2$pz, 1.22 36H(q), 2.23 6H(m), 8.89 2H(s), 1.97 6H(s); $Me_2NCN$, 1.37 36H(q), 2.43 6H(m), 1.81

(8) Shoeib, T.; El Aribi, H.; Siu, K. W. M.; Hopkinson, A. C. *J. Phys. Chem. A* **2001**, *105*, 710.
(9) Uppal, J. S.; Staley, R. H. *J. Am. Chem. Soc.* **1982**, *104*, 1235. See also: El. Aribi, H. E.; Rodriquez, C. F.; Shoeib, T.; Ling, Y.; Hopkinson, A. C.; Siu, K. W. M. *J. Phys. Chem.* **2002**, *106*, 8798.
(10) Chen, L. Z.; Miller, J. M. *Org. Mass Spectrom.* **1992**, *27*, 883.
(11) Shearer, J.; Jackson, H. L.; Schweitzer, D.; Rittenberg, D. K.; Leavy, T. M.; Kaminsky, W.; Scarrow, R. C.; Kovacs, J. A. *J. Am. Chem. Soc.* **2002**, *124*, 11417.
(12) Ehlers, A. W.; Dapprich, S.; Vyboishchickov, S. F.; Frenking, G. *Organometallics* **1996**, *15*, 105.
(13) Toupadakis, A.; Kubas, G. J.; King, W. A.; Scott, B. L.; Huhmann-Vincent, J. *Organometallics* **1998**, *17*, 5315.
(14) Cases, M.; Frenking, G.; Durán, M.; Solà, M. *Organometallics* **2002**, *21*, 4182.
(15) A range of over 10 kcal mol$^{-1}$ was computed for the isodesmic exchange reaction IrCp(CO)(L) + IrCp(Xe)($PF_3$)=IrCp(CO)(Xe) + IrCp(L)($PF_3$). A key factor stabilizing IrCp(CO)(L) as a function of L appears to be the $\sigma$ donor ability of L. See: Gusev, D. G. *Organometallics* **2009**, *28*, 763.
(16) (a) Kubas, G. J. *Organomet. Synth.* **1986**, *3*, 264. (b) Khalsa, G. R. K.; Kubas, G. J.; Unkefer, C. J.; Van Der Sluys, L. S.; Kubat-Martin, K. A. *J. Am. Chem. Soc.* **1990**, *112*, 3866.
(17) Sasaki, T.; Nakanishi, A.; Ohno, M. *J. Org. Chem.* **1981**, *46*, 5445.
(18) Ju, T. D.; Capps, K. B.; Roper, G. C.; Hoff, C. D. *Inorg. Chim. Acta* **1998**, *270*, 488.

6H(s); 2,4,6-$MeC_6H_2CN$, 1.36 36H(q), 2.47 6H(m), 6.36 2H(s), 2.28 6H(s), 1.82 3H(s); 2,6-$F_2C_6H_3CN$, 1.38 36H(q), 2.48 6H (m), 6.28 1H(m), 6.03 2H(t); AdCN, 1.39 36H(q), 2.47 6H(m), 1.60 6H(d), 1.51 3H(m), 1.26 6H(m); AdNC, 1.37 36H(q), 2.45 6H(m), 1.75 6H(d), 1.68 3H(m), 1.29 6H(m).

**Calorimetric Measurement of AdNC-Driven Displacement of L from $Mo(P^iPr_3)_2(CO)_3L$.** In a glovebox, a solution of the target compound was prepared in 5 mL of freshly distilled toluene, and transferred via syringe into the calorimeter cell. A few milligrams of freshly sublimed AdNC were loaded into the solid sample holder of the calorimeter cell. The cell was sealed, removed from the glovebox, and loaded into a Setaram C-80 calorimeter. After thermal equilibration, the reaction was initiated and followed to completion at 30 °C. Following return to baseline, the cell was returned to the glovebox, and its contents examined by FTIR to confirm complete conversion. The reported average values are based on four to six independent determinations for the enthalpy of reaction based on solid AdNC. A value (all species solvated) was determined from the measured values and the enthalpy of solution of AdNC in toluene ($\Delta H_{soln} = 3.1 \pm 0.1$ kcal mol$^{-1}$).

**$K_{eq}$ for Binding of $N_2$ to $Mo(P^iPr_3)_2(CO)_3$.** A thermostatted medium-pressure FTIR cell with $CaF_2$ windows (Harrick Scientific) was fitted with a 40 mL stainless steel bomb, valves, pressure sensor, and a thermistor probe inserted directly into the solution. This assembly was loaded in the glovebox with 0.3050 g (0.6100 mmol) $Mo(P^iPr_3)_2(CO)_3$ and 20.0 mL of 4.0 mM $Mo(CO)_6$ in toluene. The CO-stretching frequency ($\nu_{co}$ at 1984 cm$^{-1}$) of $Mo(CO)_6$ was used in data analysis as a calibration standard to correct for increased path lengths under the higher pressures of $N_2$. Initially, the cell was pressured to ~280 psi $N_2$ at room temperature, to obtain a maximum value for the absorbance due to $Mo(P^iPr_3)_2(CO)_3(N_2)$. That maximum value was then used to calculate the relative concentrations by means of difference. The pressure was released to ~15 psi, and the temperature was incrementally varied from 336 to 284 K. Corrections were made to the observed pressure of $N_2$ because of increased toluene vapor pressure at higher temperature. Values for $K_{eq}$ were interpreted in units of atm$^{-1}$. At the end of the experiment the cell was repressurized to ~280 psi at room temperature, and the sample was again examined by FTIR spectroscopy. The resultant spectrum was ultimately compared to the initial spectrum, indicating no decomposition of the reactive $Mo(P^iPr_3)_2(CO)_3$ complex. Variable temperature FTIR spectral data are shown in the Supporting Information, Figure SF-1. Three independent experiments led to values of $\Delta H = -10.3 \pm 0.8$ kcal mol$^{-1}$ and $\Delta S = -32.2 \pm 2.6$ cal mol$^{-1}$ K$^{-1}$.

**Calorimetric Measurements of the Enthalpy of Binding of $W(P^iPr_3)_2(CO)_3(N_2)$ to $W(P^iPr_3)_2(CO)_3$.** In a representative experiment, 19.3 mg of crystalline $(\mu\text{-}N_2)[W(P^iPr_3)_2(CO)_3]_2$ was loaded into the solid compartment of a calorimeter cell. The cell was then loaded with 5 mL of toluene and then sealed under a nitrogen atmosphere. The sealed cell was taken from the glovebox and loaded into a Setaram C-80 calorimeter. After thermal equilibration, the reaction was initiated and followed to completion at 30 °C. Following return to baseline, the cell was taken back into the glovebox, and its contents examined by FTIR to confirm complete conversion to $W(P^iPr_3)_2(CO)_3(N_2)$. The reported average values are based on three independent experiments. From the measured values and the enthalpy of solution of $(\mu\text{-}N_2)[W(P^iPr_3)_2(CO)_3]_2$ in toluene under an Ar atmosphere ($\Delta H = +6.7 \pm 0.3$ kcal mol$^{-1}$), a value with all species in solution for the reaction of $(\mu\text{-}N_2)[W(P^iPr_3)_2(CO)_3]_2$ with $N_2$ to form $W(P^iPr_3)_2(CO)_3(N_2)$ was determined to be $\Delta H = -1.5 \pm 0.6$ kcal mol$^{-1}$.

**$K_{eq}$ for Binding of Pyrazine to $Mo(P^iPr_3)_2(CO)_3$.** The modified FTIR cell assembly was loaded in the glovebox with 0.1939 g (0.4 mmol) of $Mo(P^iPr_3)_2(CO)_3$, 0.5025 g (6.3 mmol) of pyrazine, and 12 mL of $C_6D_6$. The concentration of pyrazine was considered as uniform, as any changes due to reaction were small compared to experimental error. Relative concentrations of the organometallic complexes were determined by band shape analysis of the spectra (Supporting Information, Figure SF-2). The absorbance maxima of the major and minor bands were measured. Assuming a symmetrical band shape, it was determined that the absorbance of the major band at the peak maximum position of the minor band was 0.19 times the major band height. This was done by measuring the absorbance equidistant on the low wavenumber side. From this the ratio of the two bands was determined.

**Calorimetric Measurements of Nitriles.** The determination of the enthalpy of binding of a series of aromatic nitriles was carried out using a crystallized sample of $Mo(P^iPr_3)_2(CO)_3(AdCN)$ as the limiting reagent following the isonitrile displacement procedure. In a typical measurement, a few milligrams of solid $Mo(P^iPr_3)_2(CO)_3(AdCN)$ were added to a solution of the free nitrile in toluene solution in the calorimeter. Reactions were quantitative under these conditions as confirmed by FTIR spectroscopy after disassembly of the calorimeter.

**Crystallographic Analyses.** Yellow single crystals of $Mo(P^iPr_3)_2(CO)_3(AdNC)$, $Mo(P^iPr_3)_2(CO)_3(AdCN)$ and $W(P^iPr_3)_2(CO)_3(AdCN)$; orange single crystals of $W(P^iPr_3)_2(CO)_3(2,4,6\text{-}Me_3C_6H_2CN)$ and maroon single crystals of $W(P^iPr_3)_2(CO)_3(2,6\text{-}F_2C_6H_2CN)$ suitable for X-ray diffraction analyses were obtained by evaporation of a mixture of benzene and octane at 21 °C under an inert atmosphere of argon. Blue single crystals of $W(P^iPr_3)_2(CO)_3(2,6\text{-}Me_2pz)$, yellow single crystals of $W(P^iPr_3)_2(CO)_3(Me_2NCN)$, and yellow single crystals of $W(P^iPr_3)_2(CO)_3(AdNC)$ were grown from a layered solution of heptane/toluene that was placed in a −20 °C freezer for 1 month. Once separated from the mother liquor, the solid crystals were fairly air stable. Each crystal was glued onto the end of a thin glass fiber; no decomposition was observed during the data collection period.

X-ray intensity data were measured using a Bruker SMART APEX2 CCD-based diffractometer with Mo Kα radiation ($\lambda = 0.71073$ Å).[19] Raw data frames were integrated with the SAINT+ program using a narrow-frame integration algorithm.[19] Corrections for Lorentz and polarization effects were also applied with SAINT+. An empirical absorption correction based on the multiple measurement of equivalent reflections was applied using SADABS. All structures were solved by a combination of direct methods and difference Fourier syntheses, and refined by full-matrix least-squares on $F^2$ using the SHELXTL software package.[20] All non-hydrogen atoms were refined with anisotropic displacement parameters. Hydrogen atoms were placed in geometrically idealized positions and included as standard riding atoms during the least-squares refinements. Crystal data, data collection parameters, and results of the analyses are listed in Supporting Information, Tables ST-4 and ST-5.

Compounds $Mo(P^iPr_3)_2(CO)_3(AdCN)$, $Mo(P^iPr_3)_2(CO)_3(AdNC)$, $W(P^iPr_3)_2(CO)_3(2,4,6\text{-}Me_3C_6H_2CN)$, and $W(P^iPr_3)_2(CO)_3(2,6\text{-}F_2C_6H_2CN)$ crystallized in the monoclinic crystal system. For compounds $Mo(P^iPr_3)_2(CO)_3(AdCN)$, $Mo(P^iPr_3)_2(CO)_3(AdNC)$, and $W(P^iPr_3)_2(CO)_3(2,6\text{-}F_2C_6H_2CN)$ the systematic absences in the intensity data were consistent with the unique space group $P2_1/n$. With $Z = 8$, there are two formula equivalents of the molecule present in the asymmetric crystal unit for these three compounds. Compounds $Mo(P^iPr_3)_2(CO)_3(AdCN)$ and $Mo(P^iPr_3)_2(CO)_3(AdNC)$ are isomorphous and isostructural. For compound $W(P^iPr_3)_2(CO)_3(2,4,6\text{-}Me_3C_6H_2CN)$ the systematic absences in the intensity data were consistent with the unique space group $P2_1/c$.

(19) *Apex2 Version 2.2-0 and SAINT+ Version 7.46A*; Bruker Analytical X-ray System, Inc.: Madison, WI, 2007.

(20) Sheldrick, G. M. *SHELXTL Version 6.1*; Bruker Analytical X-ray Systems, Inc.: Madison, WI, 2000.

Compounds $W(P^iPr_3)_2(CO)_3(AdCN)$ and $W(P^iPr_3)_2(CO)_3$-(2,6-$Me_2$pz) crystallized in the monoclinic crystal system. For compound $W(P^iPr_3)_2(CO)_3(AdCN)$ the systematic absences in the intensity data were consistent with the unique space group $P2_12_12_1$. There is minor disorder present in the adamantyl group (atoms C51−C59) which was not modeled because of satisfactory low $R$ factors, $R_1 = 3.45\%$, in the final stages of the refinement. The carbon atoms of the disordered adamantyl group were refined with isotropic displacement parameters. For compound $W(P^iPr_3)_2(CO)_3$(2,6-$Me_2$pz) the systematic absences in the intensity data were consistent with the unique space group *Pbca*. With $Z = 16$, there are two formula equivalents of the molecule present in the asymmetric crystal unit.

Crystals of $W(P^iPr_3)_2(CO)_3(AdNC)$ and $W(P^iPr_3)_2(CO)_3$-($Me_2NCN$), recrystallized from heptane, were mounted in a nylon cryoloop from Paratone-N oil under argon gas flow, placed on a Bruker diffractometer, and cooled to 141 K using a Bruker Kryoflex cryostat located at LANL. The data for the AdNC crystal were collected on a Bruker P4/1k-CCD, while the data for the $Me_2NCN$ crystal were collected on a Bruker APEX II CCD. Both instruments were equipped with sealed, graphite monochromatized Mo Kα X-ray sources ($\lambda = 0.71073$ Å). For each of the two structures a hemisphere of data was collected employing $\varphi$ or $\omega$ scans and 0.50° frame widths. All data were corrected and absorption (SADABS)[21] and Lorentz-polarization effects. Decay of reflection intensity was monitored and corrected via analysis of redundant frames. The structures were solved using Direct methods and difference Fourier techniques. All hydrogen atom positions were idealized, and rode on the atom to which they were attached. The final refinement included anisotropic temperature factors on all non-hydrogen atoms. Structure solution, refinement, graphics, and creation of publication materials were performed using SHELXTL.[20] Additional details of data collection may be found in the Supporting Information, Tables ST-6 and ST-7.

**Computational Details.** All electronic structure calculations used the B3LYP hybrid density functional method as implemented in the Gaussian 03 suite of programs.[22] Structures were optimized using the LANL2DZ basis, LANL2DZ ECP[23] and basis for the transition-metal centers and P atoms, and the Dunning−Huzinaga D95 V[24] basis for all other atoms. Optimizations were first carried out in the gas phase to obtain the basis set superposition error (BSSE) using counterpoise calculations.[25] The structures were then reoptimized and vibrational frequencies calculated in "toluene solution" (or "THF solution") using a polarizable continuum model (PCM)[26] and UAHF radii. Computed electronic energies were corrected for zero-point energy, thermal energy, and entropic effects to obtain the corresponding thermodynamic properties $H°$ and $G°$ in solution. Adding gas-phase BSSE corrections to $H°$ provided the binding enthalpies.

When possible, starting structures were modeled after crystal structures. We found that optimized structures were dependent on initial structure guesses, pointing toward multiple local minima. It became apparent that this level of theory poorly described the conformations of the $^i$Pr groups in some of the complexes. Since this behavior complicates the direct comparison of binding enthalpies, we ran a parallel set of calculations on the corresponding $PMe_3$ compounds. As an additional test of robustness, we performed single-point calculations on all optimized $PMe_3$ structures using the MWB28 ECP and basis[27] for Mo (MWB60 ECP and basis[27] for W) containing one set of f functions, and the 6-311G(d,p) 5d basis[28] for all other elements. The polarization functions in the larger basis sets can, in principle, better describe the delicate balance between $\sigma$ donation and $\pi$ backdonation. Finally, TD-B3LYP calculations were carried out on most of the $P^iPr_3$ solution-phase structures.

## Results

**Enthalpies of Ligand Binding.** Previous ligand binding studies have focused mainly on the cyclohexyl phosphine complexes $M(PCy_3)_2(CO)_3$ (M = Cr, Mo, W),[29] although some data on the more soluble isopropyl phosphine complexes have been reported.[30] For the N-donor ligands studied here, several techniques were used to assemble experimental data: calorimetric studies of ligand binding and displacement, variable temperature equilibrium studies, as well as ligand competition equilibrium studies at fixed temperature. These data and how they were derived are presented separately and then combined later to form a stability series (see Table 4) for comparison to computational data.

**Enthalpies of Reaction with 1-Adamantyl Isocyanide.** Calorimetric measurements were made of the enthalpy of displacement of weakly bound NX ligands by AdNC as shown in reaction 1 and summarized in Supporting Information, Table ST-1.

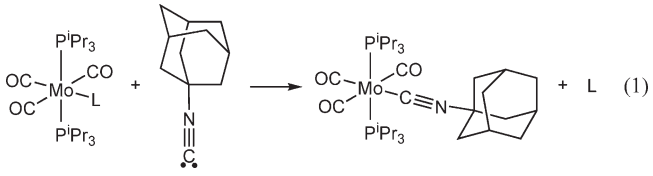

(1)

In a typical measurement, a few milligrams of solid AdNC (recrystallized and sublimed) were added to a solution of the complex in the calorimeter. Reaction is rapid and quantitative under these conditions. The enthalpy of binding of AdNC to $Mo(P^iPr_3)_2(CO)_3$, as

(21) Sheldrick, G. *SADABS 2.10*; University of Göttingen: Göttingen, Germany, 2001.
(22) Frisch, M. J. et al. *Gaussian 03*, revision D.01; Gaussian, Inc.: Wallingford, CT, 2004.
(23) (a) Hay, P. J.; Wadt, W. R. *J. Chem. Phys.* **1985**, *82*, 270. (b) Wadt, W. R.; Hay, P. J. *J. Chem. Phys.* **1985**, *82*, 284. (c) Hay, P. J.; Wadt, W. R. *J. Chem. Phys.* **1985**, *82*, 299.
(24) Dunning, T. H. Jr., Hay, P. J. In *Modern Theoretical Chemistry*; Schaefer, H. F., III, Ed.; Plenum: New York, 1976; Vol. *3*, pp 1−28.
(25) (a) Simon, S.; Duran, M.; Dannenberg, J. J. *J. Chem. Phys.* **1996**, *105*, 11024. (b) Boys, S. F.; Bernardi, F. *Mol. Phys.* **1970**, *19*, 553.
(26) (a) Miertus, S.; Scrocco, E.; Tomasi, J. *Chem. Phys.* **1981**, *55*, 117. (b) Miertus, S.; Scrocco, E.; Tomasi, J. *Chem. Phys.* **1981**, *55*, 117. (c) Mennucci, B.; Tomasi, J. *J. Chem. Phys.* **1997**, *106*, 5151.
(27) (a) Andrae, D.; Haeussermann, U.; Dolg, M.; Stoll, H.; Preuss, H. *Theor. Chim. Acta* **1990**, *77*, 123. (b) Martin, J. M. L.; Sundermann, A. *J. Chem. Phys.* **2001**, *114*, 3408.
(28) (a) McLean, A. D.; Chandler, G. S. *J. Chem. Phys.* **1980**, *72*, 5639. (b) Krishnan, R.; Binkley, J. S.; Seeger, R.; Pople, J. A. *J. Chem. Phys.* **1980**, *72*, 650.
(29) (a) McDonough, J. E.; Mendiratta, A.; Curley, J. J.; Fortman, G. C.; Fantasia, S.; Cummins, C. C.; Rybak-Akimova, E. V.; Nolan, S. P.; Hoff, C. D. *Inorg. Chem.* **2008**, *47*, 2133. (b) Weir, J. J.; McDonough, J. E.; Fortman, G.; Isrow, D.; Hoff, C. D.; Scott, B.; Kubas, G. J. *Inorg. Chem.* **2007**, *46*, 652. (c) McDonough, J. E.; Weir, J. J.; Sukcharoenphon, K.; Hoff, C. D.; Kryatova, O. P.; Rybak-Akimova, E. V.; Scott, B. L.; Kubas, G. J.; Mendiratta, A.; Cummins, C. C. *J. Am. Chem. Soc.* **2006**, *128*, 10295. (d) Lang, R. F.; Ju, T. D.; Kiss, B.; Hoff, C. D.; Bryan, J. C.; Kubas, G. J. *J. Am. Chem. Soc.* **1994**, *116*, 7917. (e) Kubas, G. J.; Burns, C. J.; Khalsa, G. R. K.; Van Der Sluys, L. S.; Kiss, G.; Hoff, C. D. *Organometallics* **1992**, *11*, 3390. (f) Zhang, K.; Gonzalez, A. A.; Mukerjee, S. L.; Chou, S. J.; Hoff, C. D.; Kubat-Martin, K. A.; Barnhart, D.; Kubas, G. J. *J. Am. Chem. Soc.* **1991**, *113*, 9170. (g) Gonzalez, A. A.; Hoff, C. D. *Inorg. Chem.* **1989**, *28*, 4285. (h) Gonzalez, A. A.; Hoff, C. D. *Inorg. Chem.* **1989**, *28*, 4295. (i) Gonzalez, A. A.; Zhang, K.; Nolan, S. P.; de la Vega, R. L.; Mukerjee, S. L.; Hoff, C. D.; Kubas, G. J. *Organometallics* **1988**, *7*, 2429. (j) Gonzalez, A. A.; Mukerjee, S. L.; Chou, S. L.; Kai, Z.; Hoff, C. D. *J. Am. Chem. Soc.* **1988**, *110*, 4419.
(30) Data on thermochemistry of $P^iPr_3$ can be found in ref 29 (e) and: Bender, B. R.; Kubas, G. J.; Jones, L. H.; Swanson, B. I.; Eckert, J.; Capps, K. B.; Hoff, C. D *J. Am. Chem. Soc.* **1997**, *119*, 9179.

**Scheme 1.** Enthalpies of Binding of Pyrazine as Mononuclear and Bridging Forms

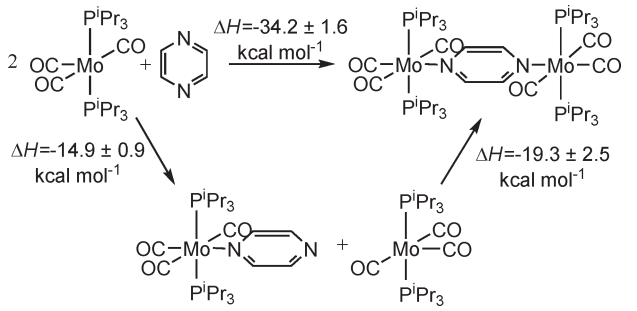


shown in reaction 2, was measured as a reference point and gave $\Delta H = -29.0 \pm 0.3$ kcal mol$^{-1}$ with all species in toluene solution.

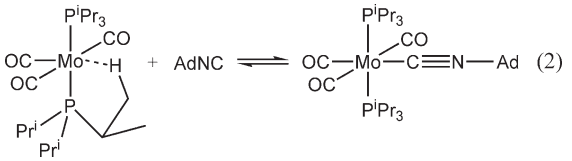


Since reaction 2 involves displacement of a C−H agostic bond with an estimated bond strength of $7 \pm 3$ kcal mol$^{-1}$ (see later discussion), this value must be added on to obtain estimates of the absolute Mo-ligand bond strength.

**Enthalpy of Binding of Pyrazine for Mononuclear and Bridging Forms.** The enthalpy of reaction of pyrazine with 2 equiv of $Mo(P^iPr_3)_2(CO)_3$ to form $\mu$-$(C_4H_4N_2)$[$Mo(P^iPr_3)_2(CO)_3]_2$ was measured by reaction with AdNC as $-34.2 \pm 1.6$ kcal mol$^{-1}$ as shown in Supporting Information, Table ST-1. This corresponds to the **sum** of the enthalpies of binding to form the mononuclear complex $(C_4H_4N_2)Mo(P^iPr_3)_2(CO)_3$ followed by its reaction to form the dinuclear complex $\mu$-$(C_4H_4N_2)$[$Mo(P^iPr_3)_2(CO)_3]_2$. The difference between these two enthalpies of binding can be determined by the equilibrium shown in reaction 3.

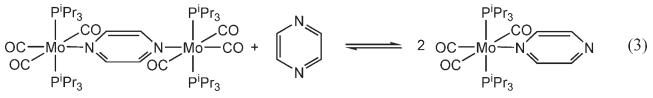


The bridging complex is favored over the monometallic species, and large excesses of pyrazine are required to produce detectable amounts of the mononuclear adduct. Variable temperature FTIR studies of reaction 3 yielded $K_{eq}$ as a function of temperature as shown in Supporting Information, Figure SF-2 from which it was determined that $\Delta H = +4.4 \pm 0.2$ kcal mol$^{-1}$ and $\Delta S = +5.8 \pm 0.3$ cal mol$^{-1}$ K$^{-1}$. The enthalpy of reaction 3, when combined with the enthalpy of binding of ($-34.2 \pm 1.6$ kcal mol$^{-1}$) for $\mu$-$(C_4H_4N_2)$[$Mo(P^iPr_3)_2(CO)_3]_2$ can be used to derive the thermochemical data shown in Scheme 1.

These data indicate that the second enthalpy of binding, $-19.3$ kcal mol$^{-1}$, is significantly stronger than the first, $-14.9$ kcal mol$^{-1}$. Since steric factors would be expected to oppose it, electronic factors must favor formation of the $\mu$-bridging dimer.

The derived data for binding of pyrazine to form the mononuclear complex, $\Delta H = -14.9 \pm 0.9$ kcal mol$^{-1}$, is in good agreement with the independently measured calorimetric value (see Supporting Information, Table S-T1) for binding of 2,6-dimethylpyrazine ($\Delta H = -14.8 \pm 0.6$ kcal mol$^{-1}$), as shown in reaction 4.

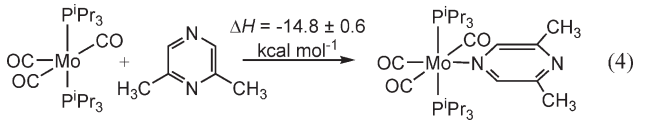


The ligand 2,6 dimethylpyrazine does not form a dinuclear complex; presumably steric factors prohibit binding to the N atom bearing ortho methyl groups. The close agreement between the derived enthalpy of binding of monodentate pyrazine and 2,6-dimethylpyrazine appears reasonable and gives support to the measured data.

**Enthalpy of Binding of $N_2$ for the Mononuclear and Bridging Forms.** Binding of $N_2$ to $Mo(P^iPr_3)_2(CO)_3$ is not quantitative, but an equilibrium is rapidly established as shown in reaction 5.

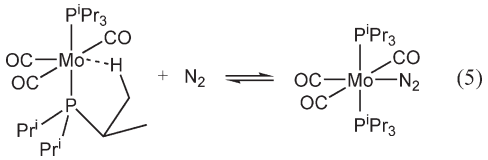


Using FTIR techniques, the value of $K_{eq}$ for this reaction was measured as a function of temperature, and the data are shown in Supporting Information, Figure SF-3.

In spite of experimental scatter in the individually measured values, due in part to the highly air-sensitive nature of the solutions, the derived thermodynamic parameters, $\Delta H = -10.3 \pm 0.8$ kcal mol$^{-1}$ and $\Delta S = -32.2 \pm 2.6$ cal mol$^{-1}$ K$^{-1}$, are in keeping with data for binding of $N_2$ to $Mo(PCy_3)_2(CO)_3$ for which we have previously found[27] $\Delta H = -9.0$ kcal mol$^{-1}$ and $\Delta S = -32.1$ cal mol$^{-1}$ K$^{-1}$. The slightly more exothermic binding of $N_2$ to the $P^iPr_3$ complex compared to the $PCy_3$ analogue has been observed for other ligands as well, and is attributed to differences in the agostic bond strength, as well as to steric factors.[31]

It was of interest to estimate the enthalpy of binding of $N_2$ in forming the bridging complex $\mu$-$(N_2)$[$Mo(P^iPr_3)_2(CO)_3]_2$, particularly for comparison to the formation of $\mu$-$(C_4H_4N_2)$[$Mo(P^iPr_3)_2(CO)_3]_2$ described above. In spite of the fact that this complex is stable as a solid, its stability in solution prevented quantitative measurement. However, the corresponding W complex is more stable, and we were able to determine the difference between the binding energies of $N_2$ in the mononuclear and bridging complexes by simple measurement of the enthalpies of solution. Dissolution of the bridging dinuclear complex under argon does not result in any reaction, and its enthalpy corresponds to reaction 6.

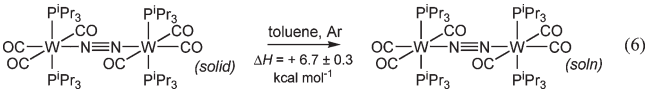


(31) Kubas, G. J.; Burns, C. J.; Khalsa, G. R. J.; Van Der Sluys, L. S.; Kiss, G.; Hoff, C. D. *Organometallics* **1992**, *11*, 3390.

In contrast, dissolution of the bridging complex under 1 atm $N_2$ results in quantitative conversion to the mononuclear complex as shown in reaction 7.

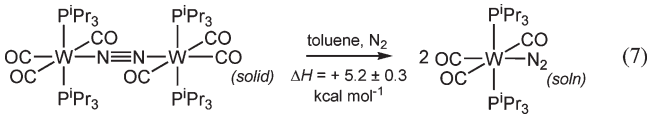

(7)

Subtracting reaction 7 from reaction 6 yields a $\Delta H = +1.5 \pm 0.6$ kcal mol$^{-1}$ for reaction 8.

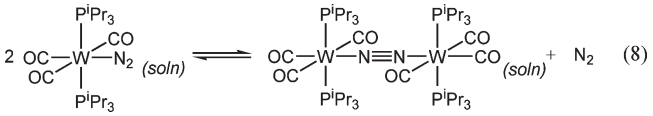

(8)

Assuming a similar behavior for Mo and W,[32] we estimate a value of $-8.8 \pm 1.2$ kcal mol$^{-1}$ for the enthalpy of binding of $Mo(P^iPr_3)_2(CO)_3(N_2)$ to form the bridging species.

**Binding of Nitriles: Calorimetric and Spectroscopic Data.** As shown in the data in Supporting Information, Table ST-1, the difference in enthalpy of binding of benzonitrile and the alkyl nitriles acetonitrile and adamantyl nitrile is only $1.0 \pm 0.5$ kcal mol$^{-1}$. Because of the exothermic nature of the reactions with AdNC, it was decided that more accurate data for a range of nitriles might be obtained by measuring the smaller enthalpy of reaction when an arene nitrile displaces adamantyl nitrile as shown in reaction 9.

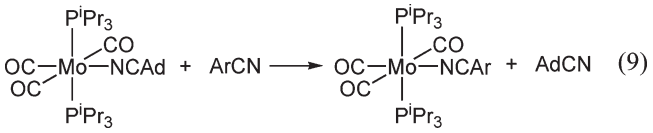

(9)

In these reactions, the readily prepared and purified AdCN complex, the structure of which is shown in Supporting Information Figure SF-4, was used as the limiting reagent and the experimental enthalpy of reaction measured in its reactions with excess ArCN. The measured enthalpies of these reactions for a set of substituted benzonitriles (Ar = 4-$NMe_2C_6H_4$; 2,4,6-$Me_3C_6H_2$; 2,6-$F_2C_6H_3$; 4-$CF_3C_6H_4$; $F_5C_6$) were all small, and the procedural dilution of the polar nitriles was found to play a role in the calorimetric measurements nearly as significant as the reactions themselves. The enthalpies measured experimentally for reaction 9 for a series of benzonitriles, as well as the derived enthalpies of binding, are collected in Table 1.

Because the entire enthalpy range was $< 1$ kcal mol$^{-1}$, the bond strengths in solution indicate only a small dependence of the Mo−N bond on R in the complexes. As shown in Figure 1, this limited range of bond strengths is accompanied by a dramatic change in color for these adducts. Spectroscopic data are summarized in Supporting Information, Table ST-2.

(32) Work on related ligand binding shows that enthalpies of binding of Mo and W closely resemble each other, with binding to Mo being $\approx 0.9$ times that of W. Because of the low value of this difference, and the high experimental error, no change was made. Under 1 atm of $N_2$ pressure we see no evidence for any of the dinuclear complex in solution, only terminal binding and unsaturated complex were detected by FTIR.

**Enthalpy of Binding of Dimethylcyanamide and Ethyldiazoacetate.** Because of low solubility of the complexes formed, it was difficult to make reliable calorimetric measurements for the enthalpies of binding of these two ligands. Instead, estimates of $K_{eq}$ for binding of ligands near to them in bond strength were carried out. Quantitative FTIR studies at room temperature showed that the values for $K_{eq}$ for reactions 10 and 11 are $7 \pm 2$ and $5 \pm 2$, respectively.

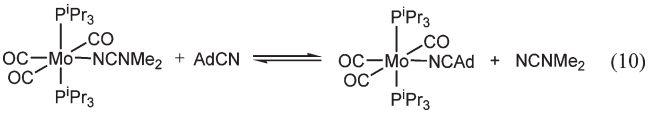

(10)

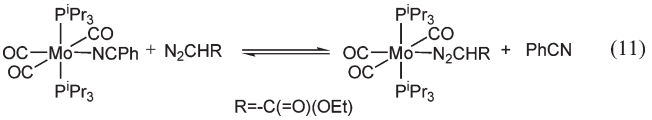

(11)

This corresponds to values of $\Delta G$ at 298 K of $-1.2 \pm 0.3$ and $-1.0 \pm 0.3$ kcal mol$^{-1}$ for reactions 10 and 11, respectively. This implies that $Me_2NCN$ has a free energy of binding 1.2 kcal mol$^{-1}$ weaker than AdCN, and that $N_2C(H)C(=O)OEt$ has a free energy of binding 1.0 kcal mol$^{-1}$ stronger than benzonitrile. The free energy changes are attributed to be primarily due to enthalpic rather than entropic factors, an approximation that is likely valid within experimental errors for these reactions.[33]

**Quinuclidine.** It is known that primary and secondary amines bind to the Kubas complexes, but tertiary amines do not.[34] This is typically ascribed to steric factors at the sterically crowded metal center which prohibit binding of bulky amines. Even in the presence of a large excess of quinuclidine, no detectable complex was observed at room temperature.

**X-ray Structure Determinations.** Crystal structures of $W(P^iPr_3)_2(CO)_3$(2,4,6-$Me_3C_6H_2CN$), $W(P^iPr_3)_2(CO)_3$(2,6-$Me_2$pz), and $W(P^iPr_3)_2(CO)_3(Me_2NCN)$ are shown in Figures 2−4. Additional structures are shown in the Supporting Information Figures SF-3 (M = Mo; L = AdNC), SF-4 (W = Mo; L = AdNC), SF-5 (M = Mo; L = AdCN), SF-6 (M = W; L = AdCN), and SF-7 (M = W; L = 2,6-$F_2C_6H_2CN$).

Tables 2 and 3 recapitulate the highlighted bond distances and angles of the X-ray crystal structures, and compare them to computational results. Universally, the overall mononuclear geometries were slightly distorted octahedra. The $^i$Pr groups show two "axial" and one "equatorial" geometries per phosphine. The rotation of such groups, as well as the absolute stereochemistry of each "axial" $^i$Pr, is not uniform across the ligand spectrum. This is consistent with the distortions, as complexes must accommodate the ligands and this involves a non-negligible steric component. This is also consistent with the non-binding of quinuclidine; such a ligand is so bulky

(33) Estimation of the entropy of ligand substitution of 4-$CF_3C_6H_4C{\equiv}N$ and $Mo(P^iPr_3)_2(CO)_3$(4-$Me_2NC_6H_4CN$) yielded an estimate of $\Delta S° = -5 \pm 2$ cal mol$^{-1}$ K$^{-1}$. At room temperature this corresponds to about 1.5 kcal mol$^{-1}$ in terms of free energy. The error limits on $\Delta H°$ derived in this way were increased by this amount.

(34) Wasserman, H. J.; Kubas, G. J.; Ryan, R. R. *J. Am. Chem. Soc.* **1986**, *108*, 2294.

**Table 1.** Enthalpies of Binding (kcal mol$^{-1}$) Determined by Reaction of $Mo(P^iPr_3)_2(CO)_3(AdCN)$ with Several Benzonitriles (Reaction 9)

| Ligand | $\Delta H_{measured}$ | $\Delta H_{binding}$[a] |
|---|---|---|
| 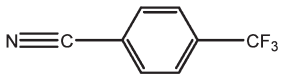 | −0.4 ± 0.1 | −17.1 ± 0.6 |
| 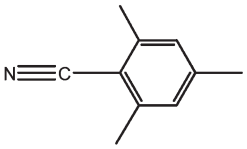 | 0.0 ± 0.1 | −16.7 ± 0.6 |
| 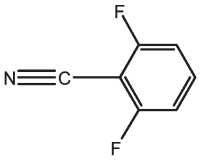 | 0.0 ± 0.1 | −16.7 ± 0.6 |
| 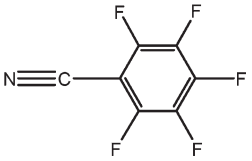 | +0.3 ± 0.1 | −16.4 ± 0.6 |
| 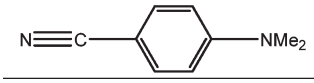 | +0.4 ± 0.1 | −16.3 ± 0.6 |

[a] Values with all species in toluene solution.

**Figure 1.** Colors of the $Mo(P^iPr_3)_2(CO)_3(RCN)$ complexes studied. From left to right: R = Ad; 4-$NMe_2C_6H_4$; 2,4,6-$Me_3C_6H_2$; $C_6H_5$; 2,6-$F_2C_6H_3$; 4-$CF_3C_6H_4$; $F_5C_6$.

that its mild $\sigma$-donor properties are overwhelmed. As is the case with most low-valent Mo and W complexes, derivatives with the same ligand produced nearly identical crystal structures.

In agreement with the solution calorimetric data, the R group of RCN did not introduce large differences in the length of the C≡N bond. The largest differences were observed between $W(P^iPr_3)_2(CO)_3(AdCN)$ (1.153(6) Å) and $Mo(P^iPr_3)_2(CO)_3(AdCN)$ (1.140(4) Å). Both values are similar to those of 1.153(6) and 1.158(6) Å for *trans*-(2,4,6-$Me_3C_6H_2CN)_2Mo(N[^iPr]Ar)_3$,[36] and 1.140(9) Å *fac*-$W(dppm)(CO)_3(CH_3CN)$.[37]

Comparison of the structures of bound nitriles to the free nitriles in the condensed phase reveals only a minimal lengthening of the C≡N bond. X-ray crystal structures report 1.139(4) Å for AdCN[38] (bound C≡N distances:

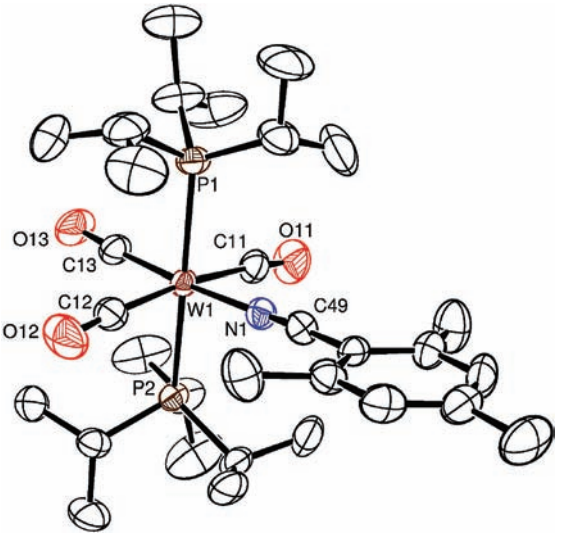


**Figure 2.** ORTEP diagram of $W(P^iPr_3)_2(CO)_3(2,4,6\text{-}Me_3C_6H_2CN)$ showing 35% probability thermal ellipsoids. Hydrogen atoms are omitted for clarity. Selected bond lengths and angles are given in Tables 2 and 3.

1.140(4) Å [Mo] and 1.153(6) [W]) and 1.141 Å for 2,6-$F_2C_6H_3CN$[39] (bound C≡N distance: 1.145(9) Å [W]). In the case of 2,4,6-$Me_3C_6H_2CN$, the C≡N bond length is 1.160 Å.[40] This is significantly longer than the C≡N bond length to 1.145(6) Å [W] in the bound complex. The reason for this apparent strengthening of the C≡N bond is unknown and is contrary to the FTIR spectral data. It has been noted that for the $\mu$-$(N_2)[W(CO)_3(P^iPr_3)_2]_2$

(36) Tsai, Y.-C.; Stephens, F. H.; Meyer, K.; Mendiratta, A.; Gheorghiu, M. D.; Cummins, C. C. *Organometallics* **2003**, *22*, 2902.
(37) Darensbourg, D. J.; Zalewski, D. J.; Plepys, C.; Campana, C. *Inorg. Chem.* **1987**, *26*, 3727.
(38) Gibbons, C. S.; Trotter, J. *Can. J. Chem.* **1973**, *51*, 87.
(39) Britton, D. *Acta Crystallogr., Sect. E* **2004**, *60*, 2189.
(40) Britton, D. *Cryst. Struct. Commun.* **1979**, *8*, 667.

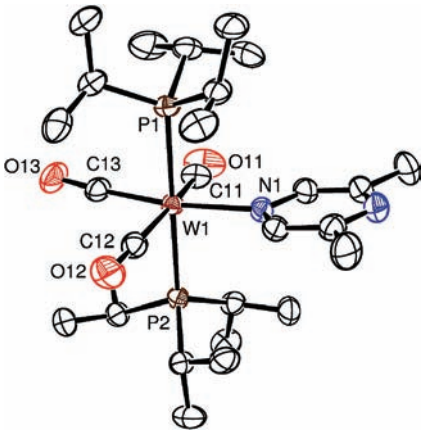


**Figure 3.** ORTEP diagram of $W(P^iPr_3)_2(CO)_3(2,6\text{-}Me_2pz)$ showing 35% probability thermal ellipsoids. Hydrogen atoms are omitted for clarity. Selected bond lengths and angles are given in Tables 2 and 3.

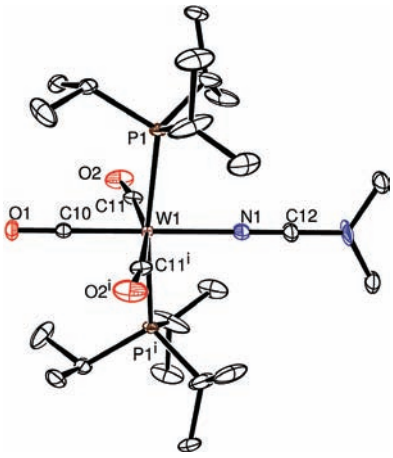


**Figure 4.** ORTEP diagram of $W(P^iPr_3)_2(CO)_3(Me_2NCN)$ showing 35% probability thermal ellipsoids. Hydrogen atoms are omitted for clarity. Selected bond lengths and angles are given in Tables 2 and 3. In spite of repeated attempts, we were not able to grow crystals of $\mu$-$(C_4H_4N_2)[M(P^iPr_3)_2(CO)_3]_2$ (M = Mo, W). The structure of the bridging complex $\mu$-$(N_2)[W(P^iPr_3)_2(CO)_3]_2$ has been reported.[35] Selected experimental and computed (see later section) bond distances and angles of X-ray crystal structures that were determined are listed in Tables 2 and 3.

complex the N≡N distance is 1.136(6) Å, suggesting that electron donation into $\pi^*_{NN}$ is minimal.[41] This was explained in terms of resonance structures in which the W−N≡N−W (not W≡N−N≡W) dominated. For W−N≡C−R, no stable resonance structure can be drawn. Thus, it may be that backbonding is hampered by a lack of resonance within the ligand itself.

Steric interactions with the phosphines seem not to play a large role in nitrile binding. The CN may be thought of as a "spacer" between two bulky groups. In fact, the shortest W−N bond lengths were observed for benzonitriles with electron-withdrawing fluorine substituents in the *ortho* position. The W−N distance was 2.130(6) Å for $2,6\text{-}F_2C_6H_2CN$ and 2.166(4) Å for $2,4,6\text{-}Me_3C_6H_2CN$, but 2.192(5) Å for $Me_2NCN$. This is consistent with the backbonding being enhanced by the electron-withdrawing fluorines. The M−N bond distances for the complexes with nitrile adducts are consistent with literature values: 2.190(5) Å in *fac*-$W(dppm)(CO)_3(CH_3CN)$,[37] 2.227(12) and 2.204(12) Å for two separate forms of $W(CO)_5(AdCN)$,[42] and 2.21 Å in $W(CO)_3(CH_3CN)_3$.[43]

The most remarkable feature of $W(P^iPr_3)_2(CO)_3(Me_2NCN)$ is that the amide N exhibits trigonal planar geometry. This behavior has been previously reported for other complexes such as $Cr(CO)_5(NCNEt_2)$,[44] *trans*-$[Fe(Et_2PCH_2CH_2PEt_2)_2(NCNEt_2)_2][BF_4]_2$,[45] and *trans*-$Mo(Ph_2PCH_2CH_2PPh_2)_2(NCNEt_2)(N_2)$.[46] This geometric preference for trigonal planar geometry of the amide is attributed to delocalization of the amide lone pair of electrons and significant contribution of the $sp^2$ hybridized N resonance form as shown in reaction 12.

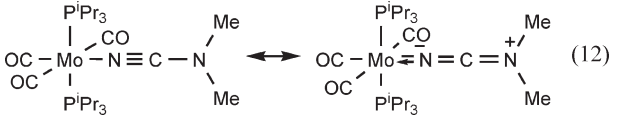


(12)

Structures of the AdNC complexes are shown in the Supporting Information, Figures SF-3 and SF-4. As expected, the M−C bonds (2.139(3) Å in the Mo complex; 2.113(6) Å in the W complex) are much shorter than the M−N (2.220(3) Å in the Mo complex; 2.195(4) Å in the W complex) bond of the nitrile complexes. This reflects increased $\sigma$-basicity and $\pi$-acidity of the isonitrile. Carbon is a poorer electrophile than N, and thus a stronger electron $\sigma$-donor. For a similar reason the $\pi^*$ lobes centered on the C of the isonitrile are larger than those of the analogous $\pi^*$ lobes centered on N of the nitrile. This results in a more favorable overlap with the metal d orbitals in the isonitrile compared to the nitrile and thus stronger backbonding. Both the W−C bond and the N≡C bond are consistent with similar literature values: $CpW(CO)_3(\mu\text{-}PPh_2)W(CO)_4(^iPrNC)$[47] ($R$(W−C) = 2.144(11) Å, $R$(N≡C) = 1.139(13) Å), *cis*-$W(\eta^1\text{-}dppm)(CO)_4(C_6H_5NC)$[48] ($R$(W−C) = 2.133(8) Å, $R$(N≡C) = 1.117(10) Å), $Mo(CO)_3(^tBuNC)_3$[49] ($R$(Mo−C) = 2.140(4), 2.148(4), and 2.156(4) Å, $R$(N≡C) = 1.159(5), 1.162(5), and 1.146(6) Å).

It is also worth noting that Tutt and Zink have reported[50] a W−N bond length of 2.26(1) Å for the structure of $W(CO)_5(C_5H_5N)$ which is nearly identical to the W−N distance in the $2,6\text{-}Me_2pz$ structure. A single crystal X-ray structure has also been reported for the free $2,6\text{-}Me_2pz$ ligand.[51] Binding of the $2,6\text{-}Me_3N_2C_4H_2$ does not significantly alter the geometry of the ligand.

(41) Butts, M. D.; Bryan, J. C.; Lou, X.-L.; Kubas, G. J. *Inorg. Chem.* **1997**, *36*, 3341.

(42) Jefford, V. J.; Schriver, M. J.; Zaworotko, M. J. *Can. J. Chem.* **1996**, *74*, 107.

(43) Hamilton, E. J. M.; Smith, D. E.; Welch, A. J. *Acta. Crystallogr., Sect.C: Cryst. Struct. Commun.* **1987**, *43*, 1214.

(44) Ohnet, M. -N.; Spasojevic-de Brie, A.; Dao, N. Q.; Schweiss, P.; Braden, M.; Fischer, H.; Reindl, D. *J. Chem. Soc., Dalton Trans.* **1995**, 665.

(45) Martins, L. M. R. D. S.; Fraústo da Silva, J. J. R.; Pombeiro, A. J. L.; Henderson, R. A.; Evans, D. J.; Benetollo, F.; Bombieri, G.; Michelin, R. A. *Inorg. Chim. Acta* **1999**, *291*, 39.

(46) Cunha, S. M. P. R. M.; Guedes da Silva, M. F. C.; Pombeiro, A. J. L. *Inorg. Chem.* **2003**, *42*, 2157.

(47) Shyu, S.-G.; Singh, R.; Su, C.-J; Lin, K.-J. *Eur. J. Inorg. Chem.* **2002**, 1343.

(48) Knorr, M.; Jourdain, I.; Lentz, D.; Willemsen, S.; Strohmann, C. *J. Organomet. Chem.* **2003**, *684*, 216.

(49) Imhof, W.; Halbauer, K.; Donnecke, D.; Gorls, H. *Acta Crystallogr., Sect. E* **2006**, *62*, 462.

(50) Tutt, L.; Zink, Z. I. *J. Am. Chem. Soc.* **1986**, *108*, 5830.

(51) Kaiser-Morris, E.; Cousson, A.; Paulus, W.; Fillaux, F. *Acta. Crystallogr., Sect. E* **2001**, *57*, 1116.

**Table 2.** Selected $M(P^iPr_3)_2(CO)_3L$ Experimental and Computed (in *italics*) Bond Distances (Å)

| | M1−N1 | N1−C49 | C11−O11 | C12−O12 | C13−O13 |
|---|---|---|---|---|---|
| | | | $Mo(P^iPr_3)_2CO_3$ | | |
| AdNC | 2.139(3),[a] *2.115*[a] | 1.158(3), *1.193* | 1.147(4), *1.193* | 1.139(3), *1.196* | 1.162(4), *1.204* |
| AdCN | 2.220(3), *2.246* | 1.140(4), *1.176* | 1.147(4), *1.204* | 1.144(4), *1.197* | 1.170(4), *1.210* |
| | | | $W(P^iPr_3)_2CO_3$ | | |
| AdNC | 2.113(6),[a] *2.117*[a] | 1.171(7), *1.195* | 1.159(6), *1.200* | 1.155(6), *1.199* | 1.167(7), *1.207* |
| AdCN | 2.195(4), *2.177* | 1.153(6), *1.178* | 1.130(7), *1.202* | 1.177(8), *1.200* | 1.166(8), *1.213* |
| 2,4,6-$Me_3C_6H_2CN$ | 2.166(4), *2.133* | 1.145(6), *1.185* | 1.150(6), *1.200* | 1.168(6), *1.201* | 1.172(6), *1.210* |
| $Me_2NCN$ | 2.192(5), *2.185* | 1.151(7),[b] *1.187* | 1.178(6),[c] *1.203* | 1.178(6),[c] *1.201* | 1.165(5),[d] *1.215* |
| 2,6-$F_2C_6H_3CN$ | 2.130(6) | 1.145(9) | 1.169(10) | 1.146(11) | 1.170(10) |
| 2,6-$Me_2$pz | 2.257(4) | n/a | 1.155(6) | 1.158(6) | 1.169(6) |

[a] The ligands in these cases are isonitriles and the bond distance corresponds to M1−C49. The atoms referred to in these cases correspond to the following. [b] N1−C12. [c] C11−O2. [d] C10−O1.

**Table 3.** Selected Experimental and Computed (*in italics*) Bond Angles (deg) for $M(P^iPr_3)_2(CO)_3L$ Complexes.[a]

| | experiment and *computation* values | | | | |
|---|---|---|---|---|---|
| | M1−N1−C49 | P1−M1−P2 | N1−M1−P1 N1−M1−P2 | C11−M1−C12 | N1−M1−C11 N1−M1−C12 |
| | | | $Mo(P^iPr_3)_2CO_3$ | | |
| AdNC | 178.0(2),[b] *176.9* | 174.30(2), *176.5* | 89.05(7),[c] *91.6*<br>85.33(7),[c] *85.1* | 170.3(1), *172.8* | 94.7(1), *93.1*<br>94.9(1), *92.4* |
| AdCN | 178.4(3), *177.8* | 173.60(3), *174.8* | 88.43(7), *90.3*<br>85.24(7), *84.8* | 166.8(2), *171.9* | 96.4(1), *94.0*<br>96.8(1), *93.2* |
| | | | $W(P^iPr_3)_2CO_3$ | | |
| AdNC | 178.1(5),[b] *177.8* | 173.71(5), *175.9* | 88.2(2),[c] *91.1*<br>86.1(2),[c] *85.1* | 170.9(2), *172.8* | 96.4(2), *93.0*<br>90.6(2), *92.6* |
| AdCN | 176.9(5), *178.0* | 173.06(5), *174.2* | 86.0(1), *84.4*<br>87.2(1), *90.2* | 167.8(3), *171.3* | 98.0(3), *94.6*<br>94.2(2), *93.2* |
| 2,4,6-$Me_3C_6H_2CN$ | 175.1(4), *176.7* | 182.92(4), *178.4* | 87.5(1), *86.1*<br>94.9(1), *95.4* | 172.6(2), *172.1* | 91.5(2), *89.7*<br>86.7(2), *90.0* |
| $Me_2NCN$ | 180.0(2),[d] *178.1* | 172.25(4),[e] *174.9* | 86.13(2),[f] *84.6*<br>86.13(2),[f] *90.4* | 166.3(2)[g] *170.7* | 96.8(1),[h] *94.1*<br>96.8(1),[h] *94.2* |
| 2,6-$F_2C_6H_3CN$ | 177.6(7) | 174.64(9) | 89.2(2)<br>86.7(2) | 170.7(4) | 96.8(3)<br>90.9(4) |
| 2,6-$Me_2$pz | n/a | 179.52(4) | 86.4(1)<br>93.5(1) | 167.1(2) | 94.4(2)<br>95.6(2) |

[a] Bond angles shown by italic fonts are from values obtained from B3LYP calculations. [b] The ligands in these cases are isonitriles and the bond angle corresponds to M1−C49−N1. [c] The ligands in these cases are isonitriles and the bond angle corresponds to C49−M1−PX (X = 1,2). The bond angles in these cases refer to the following. [d] W1−N1−C12. [e] P1−W1−P1$^i$. [f] N1−W1−P1. [g] C11−W1−C11. [h] N1−W1−C10.

Kaim et al. have reported[52] the structure of $[W(PCy_3)_2(CO)_3(N\text{-}MeC_4H_4N_2)][PF_6]$. The W−N bond was reported as 2.101(10) Å. This bond length is greatly reduced from that which was determined in $W(P^iPr_3)_2(CO)_3$(2,6-$Me_2$pz) (2.257(4) Å). This difference in bond length can be attributed to the higher degree of $\pi$-back-donation from the metal fragment to the pyrazinium ligand compared to neutral 2,6-$Me_2$pz because of the stronger $\pi$-acid character of the cationic acceptor.

**Computational Results.** Computational data generated in this work can be compared directly to independent experimental determinations in the three major areas of structure, energetics, and spectroscopy. The interrelationship of these areas in assessing the nature of the Mo−NX bond is discussed later. The focus on this section is simply on assessing the correlation of these data.

Selected B3LYP optimized bond distances and angles are shown together with X-ray single-crystal diffraction results in Tables 2 and 3. As seen in the data in Tables 2 and 3, there is generally good agreement between computed and measured structures. There appears to be a tendency for the computed M−N bond distances to be slightly shorter and all other distances slightly longer than experimental. However, none of these present any significant differences, thus providing evidence that the computed structures are reliable and that the computed minimum-energy configurations are essentially correct.

The complexes that exhibited the largest structural difference between the gas phase and PCM-toluene solution were those of $AdN_3$, so we selected those complexes to investigate whether the computed gas-phase BSSEs were adequate for the solvated structures. This was done by recomputing the electronic energy of the

(35) Butts, M. D.; Bryan, J. C.; Luo, X.−L.; Kubas, G. J. *Inorg. Chem.* **1997**, *36*, 3341.
(52) Bruns, W.; Hausen, H.-D.; Kaim, W.; Schulz, A. *J. Organomet. Chem.* **1993**, *444*, 12.

**Table 4.** Experimental and Computational Binding Enthalpies (kcal mol$^{-1}$) for $M(PR_3)_2(CO)_3L$

| M | L | $\Delta H_{expt}$[a] | $\Delta H(P^iPr_3)$[b] | $\Delta H(PMe_3)$[c] | $\Delta H_{large}(PMe_3)$[d] |
|---|---|---|---|---|---|
| Mo | $H_2$ | | −2.4 | −7.3 | −11.2 |
| | $N_2$ | −10.3 ± 0.8 | −12.4 | −18.1 | −16.5 |
| | $Mo(PR_3)_2(CO)_3N_2$ | −8.8 ± 1.2 | 6.0 | −10.3 | −12.5 |
| | $N_2CHSiMe_3$ | −13.8 ± 0.5 | −11.9 | −18.6 | −17.9 |
| | $N_2CHC(=O)OEt$ | −18.6 ± 1.8[f] | −17.1 | −22.5 | −20.8 |
| | $N_3Ad$ | −11.2 ± 0.4 | −10.9 | −16.1 | −14.6 |
| | AdNC | −29.0 ± 0.3 | −21.1 | −28.9 | −30.3 |
| | $CH_3CN$ | −16.6 ± 0.4 | −10.3 | −17.3 | −17.8 |
| | AdCN | −16.7 ± 0.6 | −9.9 | −17.2 | −17.6 |
| | $C_6H_5CN$ | −17.6 ± 0.4 | −12.5 | −19.1 | −19.6 |
| | $2,4,6\text{-}Me_3C_6H_2CN$ | −16.7 ± 0.6 | −11.5 | −18.6 | −19.2 |
| | $4\text{-}NMe_2C_6H_4CN$ | −16.3 ± 0.6 | −12.2 | −18.8 | −19.2 |
| | $4\text{-}CF_3C_6H_4CN$ | −17.1 ± 0.6 | −13.5 | −20.5 | −20.7 |
| | $2,6\text{-}F_2C_6H_3CN$ | −16.7 ± 0.6 | −13.5 | −19.7 | −20.1 |
| | $C_6F_5CN$ | −16.4 ± 0.6 | −15.3 | −21.3 | −20.6 |
| | $Me_2NCN$ | −15.5 ± 1.8[i] | −10.6 | −17.6 | −17.9 |
| | Quinuclidine | n.a. | 11.2 | −7.9 | −5.9 |
| | $C_5H_5N$ (pyridine) | −17.0 ± 0.4 | −8.5 | −17.9 | −16.7 |
| | $C_4H_4N_2$ (pz) bridged | −34.2 ± 1.6[j] | | | |
| | $C_4H_4N_2$ (pz) | −14.9 ± 0.9 | −8.6 | −17.7 | −16.6 |
| | $Mo(PR_3)_2(CO)_3pz$ | −19.3 ± 2.5 | 0.3 | −13.5 | −13.0 |
| | $2,6\text{-}Me_2pz$ | −14.8 ± 0.6 | −8.7 | −17.9 | −16.8 |
| | [4-Mepz][$PF_6$] | −17.5 ± 0.8[k] | −16.7[k] | −23.6[k] | −23.2[k] |
| | THF | | −0.7[k] | −11.6[k] | −9.8[k] |
| W | $N_2$ | | −18.0 | −24.3 | −18.7 |
| | $W(PR_3)_2(CO)_3N_2$ | | 1.4 | −16.8 | −13.4 |
| | AdNC | | −28.3 | −37.5 | −35.3 |
| | AdCN | | −14.7 | −23.1 | −21.5 |
| | $2,4,6\text{-}Me_3C_6H_2CN$ | | −17.0 | −25.1 | −23.0 |
| | $Me_2NCN$ | | −15.6 | −23.5 | −21.1 |

[a] Experimental enthalpy of binding of L to $Mo(P^iPr_3)_2(CO)_3$ with all species in toluene solution unless stated otherwise. [b] Computational enthalpy of binding of L to $Mo(P^iPr_3)_2(CO)_3$. [c] Computational enthalpy of binding of L to $M(PMe_3)_2(CO)_3$. [d] Computational enthalpy of binding of L to $M(PMe_3)_2(CO)_3$ using the larger basis set. [e] Based on ligand displacement by AdNC. [f] Based on $K_{eq}$ with PhCN. [g] Determined from the reaction of $Mo(P^iPr_3)_2(CO)_3$ with AdNC. [h] Determined by reaction of $Mo(P^iPr_3)_2(CO)_3(AdCN)$ with benzonitriles. [i] Based on $K_{eq}$ with AdCN. [j] Enthalpy corresponding to the binding of both nitrogens of pyrazine to form the bridging species. [k] Measured (computed) in THF.

*optimized PCM-toluene structure* with the bulky adamantyl azide ligand *in the gas phase* as a single-point counterpoise calculation. The BSSEs for both the $Mo(P^iPr_3)_2(CO)_3(AdN_3)$ and $Mo(PMe_3)_2(CO)_3(AdN_3)$ complexes were found to be close to those of their gas-phase structure counterparts (5.4 vs 5.3 and 4.9 vs 4.5 kcal mol$^{-1}$, respectively).

Experimentally derived (see earlier section) values of $\Delta H°$ for the binding of the various ligands studied to $Mo(P^iPr_3)_2(CO)_3$ are compared to BSSE-corrected computed values, $\Delta H°_{BSSE}$, in Table 4. Also presented in Table 4 are the computed values of $\Delta H°_{BSSE}$ for binding of the same ligands to $Mo(PMe_3)_2(CO)_3$ and of selected ligands to $W(P^iPr_3)_2(CO)_3$ and $W(PMe_3)_2(CO)_3$. The calculated binding enthalpies for the complexes with $PMe_3$ ligands are listed for both the small (LANL2DZ) and large (MWB28 or MWB60 ECP and basis for the metal center; 6-311G(d,p) 5d for all other elements) basis sets.

A plot of the computational versus experimental enthalpies of binding to $Mo(P^iPr_3)_2(CO)_3$ (Figure 5) excludes two points: the $N_2$- and the pyrazine-bridged complexes, $[Mo(P^iPr_3)_2(CO)_3]_2(N_2)$ and $[Mo(P^iPr_3)_2(CO)_3]_2(C_4H_4N_2)$. These are predicted by calculations to have local minima that are unstable with respect to dissociation, in contrast to the experimental fact of their existence. This can be explained by poorly described van der Waals interactions controlling the conformations of the bulky $P^iPr_3$ groups, weak bonding with the $N_2$ and pyrazine bridging ligands, and/or steric effects.

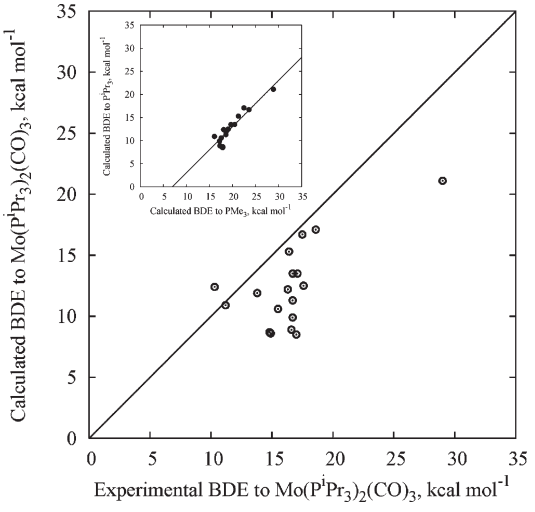


**Figure 5.** Plot of calculated N-binding bond dissociation energies (= $-\Delta H°_{bind}$) for $Mo(P^iPr_3)_2(CO)_3$ vs experimental values for $Mo(P^iPr_3)_2(CO)_3$. The line drawn is not the best fit, but a line with slope = 1 to show that most of the calculated enthalpies of binding are lower than the experimental values. (Inset) Plot of calculated BDE values for $Mo(P^iPr_3)_2(CO)_3$ vs. calculated BDE values for $Mo(PMe_3)_2(CO)_3$. The line drawn indicates BDE($^i$Pr) = BDE(Me) − 7 kcal mol$^{-1}$ (see text).

Neglecting these two points, the average deviation of the calculated from the experimental binding enthalpies is +4.0 kcal mol$^{-1}$, but there is considerable scatter in the data. As shown in Figure 5, and in Table 4, only for $N_2$ is

the computed bond dissociation energy ($= -\Delta H°_{bind}$) larger than the experimental one, a possible consequence of overestimation of steric repulsive factors for other ligands.

It is noteworthy that the six ligands for which the calculated and experimental values are in best agreement are $N_2$, $N_3Ad$, $N_2CHSiMe_3$, $C_6F_5CN$, $[4\text{-Me-pz}]^+$, and $N_2CHC(=O)OEt$, and the next-best group is 2,6-$F_2C_6H_3CN$ and 4-$CF_3C_6H_4CN$. These ligands, except for $N_2$ which is a very weak $\sigma$ donor, are all of moderate $\sigma$ donor strength and moderate to good $\pi$ acceptor strength. Binding in the complexes containing these ligands could most likely be described adequately by a basis set without great flexibility for treating subtleties in the balance between $\sigma$ donation and $\pi$ backbonding.

Computation at the small and large basis set level were performed for binding of ligands to $Mo(PMe_3)_2(CO)_3$ and data is collected in Table 4. It is evident from the inset in Figure 5 that the correlation between calculated BDE values for $Mo(P^iPr_3)_2(CO)_3$ and calculated values for $Mo(PMe_3)_2(CO)_3$ is much better than the calculated and experimental values. In fact, the correlation between the calculated values for the two complexes is well represented by the relation BDE($^i$Pr) = BDE(Me) − 7 kcal mol$^{-1}$. This indicates that the intrinsic BDEs are roughly the same and that the net BDEs differ by the dissociation energy of the agostic bond in the $^i$Pr complex which is ≈7 kcal mol$^{-1}$. As shown in Figure 6, there is a better correlation between experimental data obtained for $Mo(P^iPr_3)_2(CO)_3$ and computed data for $Mo(PMe_3)_2(CO)_3$ using the *expanded basis set*. These results indicate that polarization functions and the triple-$\zeta$ basis do, indeed, better describe the delicate balance between $\sigma$ donation and $\pi$ backbonding in these complexes. The smaller basis set appears to lack this flexibility for both the $^i$Pr and Me complexes. Since $Mo(PMe_3)_2(CO)_3$ does not have an agostic bond (estimated as ≈7 ± 3 kcal mol$^{-1}$) this is in keeping with the computed intercept of 5.5 kcal mol$^{-1}$ in Figure 6, and the generally higher computed enthalpies of binding for $Mo(PMe_3)_2(CO)_3$ as seen in Table 4. In this case, the experimental values should be adjusted upward by the agostic bond which we estimate as being ≈7 kcal mol$^{-1}$ as shown in the Supporting Information, Table ST-1 where absolute BDE values are estimated.

It should be pointed out that computation of *fac*-$Mo(PMe_3)_2(CO)_3(L)$, in which the $PMe_3$ groups are trans to each other, defies experimental measurement and can only be determined computationally. The *mer*-$Mo(PMe_3)_2(CO)_3(L)$ isomer, in which the $PMe_3$ groups are cis to each other, is the thermodynamically more stable isomer for the smaller phosphine ligand. The strong correlation in Figure 6 implies that exchanging the relatively small $PMe_3$ ligands for the sterically more demanding $P^iPr_3$ ligands does not cause significant steric repulsion to the bound ligand set studied here. The main result is to enforce the *fac* over the *mer* geometry in these systems. For bulky ligands, such as quinuclidine (see Table 4) that observation is obviated, but for the majority of ligands studied here steric repulsion appears minor.

The estimated value of the absolute binding enthalpy of AdNC to $Mo(P^iPr_3)_2(CO)_3$ of 36 kcal mol$^{-1}$ is in the range of the C≡O enthalpy of binding to $Mo(CO)_5$ of

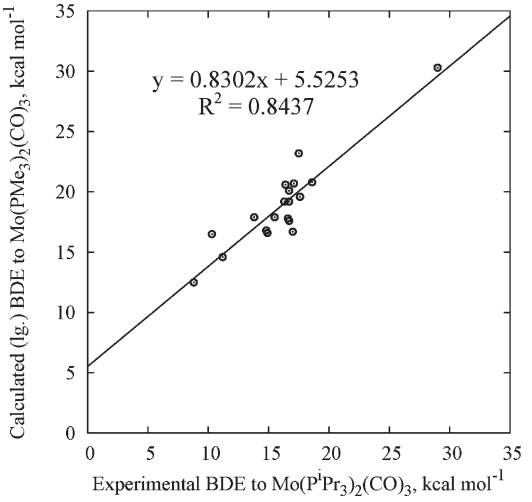


**Figure 6.** Plot of calculated N-binding enthalpies for $Mo(PMe_3)_2(CO)_3$ using a large basis set vs experimental values for $Mo(P^iPr_3)_2(CO)_3$. The line drawn is the best fit through the points. Data for the dinuclear complexes $[Mo(P^iPr_3)_2(CO)_3]_2(C_4H_4N_2)$ and $[Mo(P^iPr_3)_2(CO)_3]_2(N_2)$ are not included.

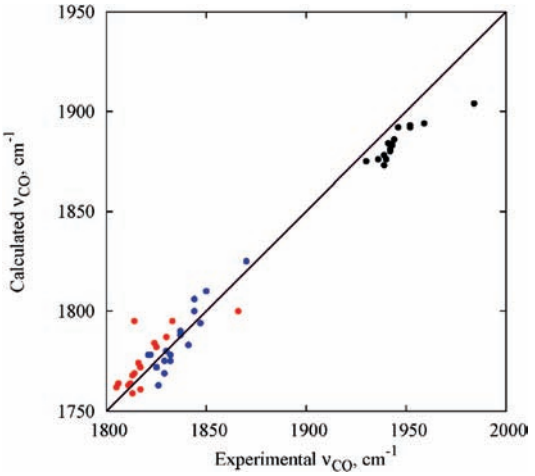


**Figure 7.** Comparison of computed and observed $\nu_{CO}$ stretching vibrations. Red points, CO stretching vibrations in normal modes that involve primarily a single CO ligand, "1 CO", and tend to have the lowest-energy CO frequencies; blue points, those that primarily involve two CO ligands, "2 CO", and tend to have intermediate-energy CO frequencies; and black points, those that involve all three CO ligands, "3 CO", and tend to have the highest-energy CO frequencies. The line indicates $\nu_{CO}(Calc) = \nu_{CO}(Expt) - 50$ cm$^{-1}$.

40 kcal mol$^{-1}$ as determined by Smith.[53] It is reasonable to expect similar enthalpies of binding of the isoelectronic RN≡C and C≡O ligands.

Computed data for UV−vis and IR spectra of M—N≡CR and M—C≡O are collected with experimental values in Supporting Information, Table ST-3. As shown in Figure 7 below, computed data are in good agreement with the trends in CO stretching frequencies, $\nu_{CO}$, but bands were offset by ≈ 50 cm$^{-1}$. Computed UV−vis spectra are shown in Supporting Information, Figure SF-9. The agreement between computed and experimental UV−vis data is shown in Figure 8. As was the case with vibrational

(53) Lewis, K. E.; Golden, D. M.; Smith, G. P. *J. Am. Chem. Soc.* **1985**, *106*, 3905.

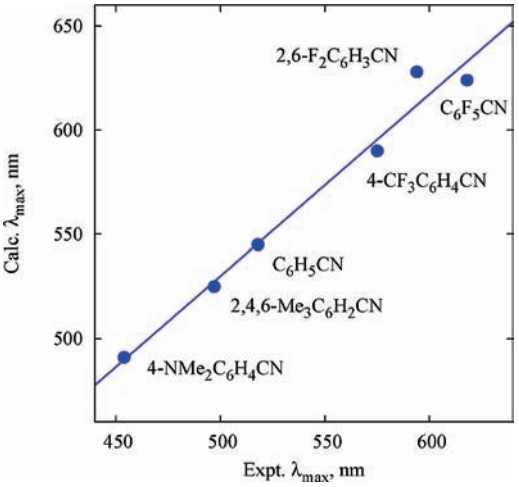


**Figure 8.** Comparison of computed and observed UV−vis absorption maxima.

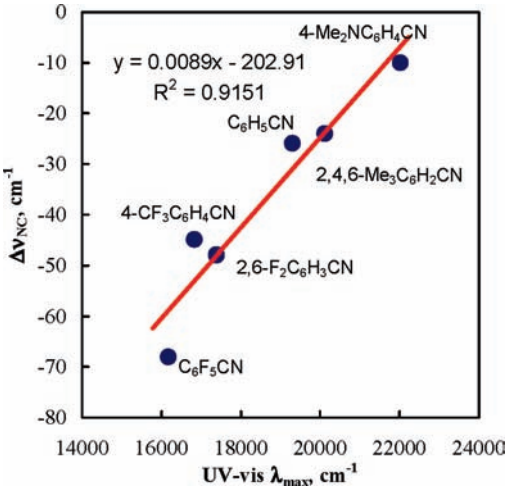


**Figure 9.** Plot of $\Delta\nu_{NC}$ vibration vs UV−vis absorbance maximum for complexes of $Mo(P^iPr_3)_2(CO)_3(N{\equiv}CAr)$ (Ar = $C_6F_5$, 2,6-$F_2C_6H_3$, 4-$CF_3C_6H_4$, 2,4,6-$Me_3C_6H_2$, $C_6H_5$, 4-$NMe_2C_6H_4$).

computations, computed UV−vis data are in excellent relative agreement with experimental observations.

## Discussion

The main goal of this work was to evaluate the range of bond energies and the nature of the bonding in $Mo(P^iPr_3)(CO)_3(NX)$. As shown in Table 4, data for W parallels that for Mo but with a more exothermic enthalpy of binding, as was also found in previous work.[4,29] In spite of the bulky nature of the phosphine ligands, structural studies show that for N≡C—R, and presumably for N═N═CHR and N═N═N—R complexes as well, steric repulsion does not play a determining role because of the presence of a "spacer" atom. It is likely that only for pyridine, pyrazine, or amine ligands that steric repulsion becomes important as can be seen by comparing the structures of W complexes of 2,4,6-$Me_3C_6H_2CN$ in Figure 3 and dimethyl pyrazine in Figure 4. There is little steric repulsion evident for the ortho-methyl groups of the nitrile. It is clear, however, that for the dimethyl pyrazine complex shown in Figure 3 binding of the N atom with ortho-methyl groups would result in severe crowding. In spite of the thermodynamic stability of the $\mu$-bridging form of pyrazine, no evidence for this was found for dimethyl pyrazine. Computation and experiment confirm that quinuclidine does not bind to $Mo(P^iPr_3)_2(CO)_3$, presumably for steric reasons since computation predicts exothermic binding to $Mo(PMe_3)_2(CO)_3$. In spite of these comments, for the ligands studied with "spacer" atoms in place, for example, N≡C—R, N═N═CHR, and N≡N—NR, it seems likely that repulsion is no more severe in their binding than it is for N≡N itself.

The most surprising result, and one which gives some insight into the role of $\pi$-bonding, is the nearly constant enthalpy of binding of arene nitriles as shown in Table 1. This is in spite of a dramatic change in color as shown in Figure 1. Accompanying the color changes and $\lambda_{max}$ are IR changes in both $\nu_{CN}$ and $\nu_{CO}$ in the complexes, all the while maintaining a nearly constant enthalpy of binding. There is a reasonable correlation between changes in the UV−vis and IR peak positions as shown in Figure 9. The larger the decrease in the nitrile stretching frequency upon coordination to the metal resulted in a longer wavelength and a darker color of the metal complexes.

The spectroscopic changes depicted in Figure 9 are indicative of $\pi$-backbonding effects becoming increasingly important in the order: 4-$Me_2N{-}C_6H_4CN$ < 2,4,6-$Me_3C_6H_2CN$ < $C_6H_5CN$ < 2,6-$F_2C_6H_3CN$ ≈ 4-$CF_3C_6H_4CN$ < $C_6F_5CN$. This order is opposite to what would be expected for $\sigma$-donor ability, as judged by gas-phase proton affinity (PA). We could not find experimental literature data for $C_6F_5CN$ (this is what is in Table 4), so we have computed the gas-phase PA to be 179.6 kcal $mol^{-1}$. The computed value for $C_6H_5CN$ was 200.2 kcal $mol^{-1}$, which is in reasonable agreement with the experimental value of 193.9 kcal $mol^{-1}$.[54] The difference in PA of benzonitrile and perfluoronitrile is thus on the order of 20 kcal $mol^{-1}$ favoring benzonitrile. Differences in binding enthalpies on that order of magnitude would not be expected in the mildly exothermic overall binding to Mo; however, the near constant values shown in Table 1 indicate that gains in $\pi$-backbonding are compensated for by losses in $\sigma$ donation, indicating a roughly equal importance for nitrile binding to $Mo(P^iPR_3)_2(CO)_3$.

Since steric factors can also play a role, a further comparison is to examine the binding of 4-$NMe_2C_6H_4CN$ and 4-$CF_3C_6H_4CN$ as ligands since the group in the *para* position should not alter the steric interactions significantly. It was found that 4-$CF_3C_6H_4CN$ bound more exothermically, yielding a computed value of $\Delta H^\circ = -0.8 \pm 0.2$ kcal $mol^{-1}$ for the reaction shown in reaction 13.

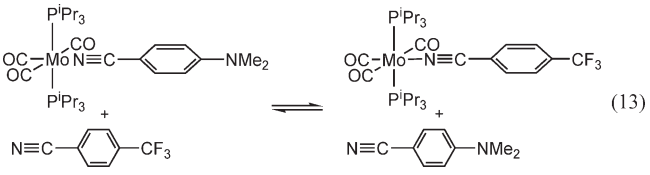


FTIR spectroscopic studies showed that at 20 °C in toluene solution, $K_{eq} = 0.3 \pm 0.2$ for the reaction shown in reaction 13, which corresponds to a value of $\Delta G^\circ = +0.7 \pm 0.3$ kcal $mol^{-1}$. This generates an estimated value of $\Delta S^\circ = -5 \pm 2$ cal $mol^{-1}$ $K^{-1}$ for the nitrile substitution reaction. A low value for the entropy of exchange would be expected and is observed. There is an apparent increase in backbonding to the nitrile ligand since, as

(54) Afeefy, H. Y.; Liebman, J. F.; Stein, S. E. Neutral Thermochemical Data. In *NIST Chemistry WebBook, NIST Standard Reference Database Number 69*; Linstrom, P. J., Mallard, W. G., Eds.; National Institute of Standards and Technology: Gaithersburg, MD, June 2005; U.S. Patent 20899 (http://webbook.nist.gov).

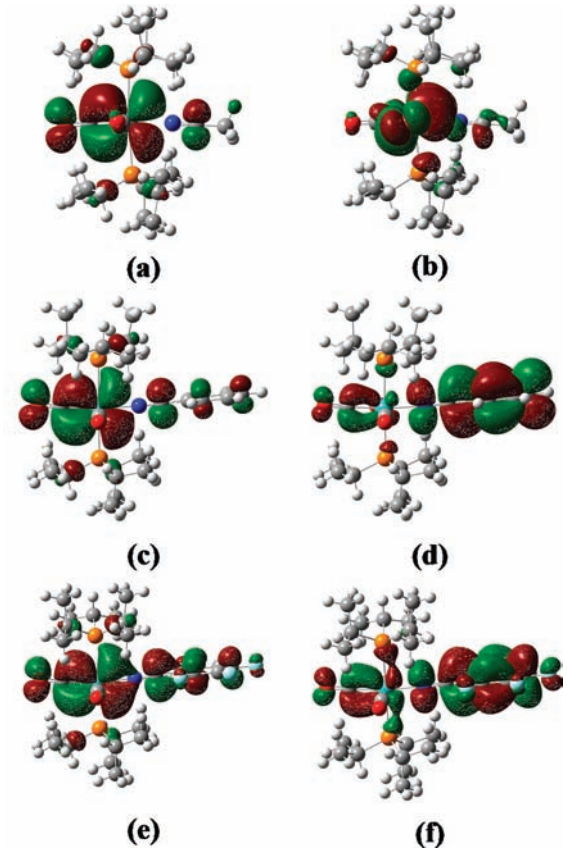


**Figure 10.** Selected HOMO (left) and LUMO (right) orbitals for Mo($P^iPr_3$)$_2$(CO)$_3$(N≡C-R) Complexes (R = $CH_3$ (a and b), $C_6H_5$ (c and d), and $C_6F_5$ (e and f). HOMO and LUMO orbitals for all complexes can be viewed in the Supporting Information, Figure SF-8.

shown in the Supporting Information, Table ST-2, the difference between coordinated nitrile and free nitrile changes from 10 $cm^{-1}$ for the 4-$NMe_2C_6H_4CN$ ligand to 45 $cm^{-1}$ for the 4-$CF_3C_6H_4CN$ ligand. Concomitant with that change, however, there is a rise in average CO frequency of about 10 $cm^{-1}$. A simple interpretation would be that the gain in backbonding to the nitrile is offset by a loss in backbonding to the CO ligand.

The nature of the $\pi$-bonding in nitriles is more complex than the spectroscopic data shown in Figure 9 imply. Computed highest occupied molecular orbitals (HOMOs) and lowest unoccupied molecular orbitals (LUMOs) for the Mo complexes of $CH_3CN$, $C_6H_5CN$, and $C_6F_5CN$ are shown in Figure 10.

It is more difficult to assess the role of $\pi$-bonding in nitriles since the frontier $\pi^*$ orbital no longer has its dominant lobe adjacent to the metal. The HOMO to LUMO transition shown in Figure 10 for N≡C−$CH_3$ appears to be largely localized on the metal. In going from N≡C−$C_6H_5$ to N≡C−$C_6F_5$, the HOMO shows increasing contribution of $\pi^*$ orbitals of the arene and the LUMO shows increasing contribution of metal based orbitals. The result is that the optical transition in Mo($P^iPr_3$)$_2$(CO)$_3$(N≡C−$C_6F_5$) shows less charge-transfer character in the sense that the difference between HOMO and LUMO net electron densities has been decreased relative to Mo($P^iPr_3$)$_2$(CO)$_3$(N≡C$CH_3$). Examination of nitrile stretching frequencies alone could lead to underestimation of the extent of $\pi$-backbonding nitrile ligand since part of the backbonding is into the arene antibonding orbital.

**Scheme 2.** Enthalpies (kcal $mol^{-1}$) of Ligand Substitution Viewed As Carbene Transfer

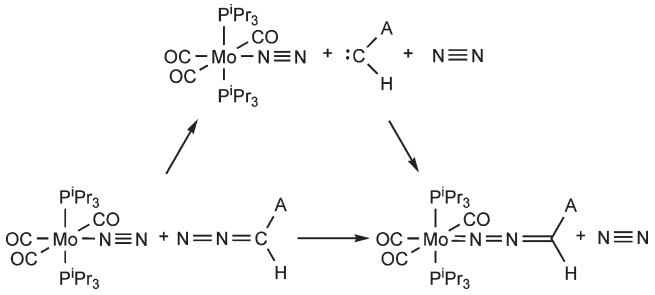

Additional evidence for the role of $\pi$-backbonding is found in enthalpies of binding of N≡N—X ligands which contain (in at least one hybrid resonance form) a formal N≡N bond. Experimental binding enthalpies spanned 10 kcal $mol^{-1}$: Mo($P^iPr_3$)$_2$(CO)$_3$($N_2$) < $N_2$ < $N_3$Ad < $N_2$CHSi$Me_3$ < $N_2$-CHC(=O)OEt (Table 4). Experimental displacement of $N_2$ is exothermic by 3.5 kcal $mol^{-1}$ for $N_2$CHSi$Me_3$ and by 8.3 kcal $mol^{-1}$ for $N_2$CHC(=O)OEt. These reactions may be viewed (from a thermodynamic perspective) as carbene transfers (Scheme 2).

In this view, the increased electron density on the uncoordinated lone pair of complexed $N_2$ would make it more basic and form a better bond to an electrophillic carbene relative to free $N_2$. Interestingly, the CO stretch of $N_2$CHC(=O)OEt exhibits a bathochromic shift upon coordination to the metal fragment. This is in keeping with increased single-bond character of the CO bond as a result of the resonance form on the right shown in reaction 14. The somewhat surprising delocalization from Mo to the carbonyl oxygen of $N_2$CHC(=O)OEt is also apparent in the HOMO shown in the Supporting Information, Figure SF-8. This type of delocalization may be responsible for the surprisingly high stability of this bound carbene.

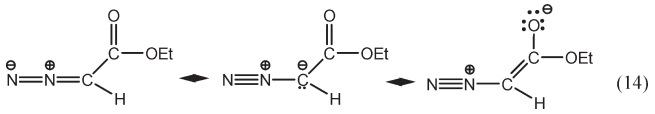

(14)

**N-heterocyclic Ligands.** Quinuclidine does not bind to the Mo($P^iPr_3$)$_2$(CO)$_3$ complex, but computation says that it *should* bind to the less bulky Mo($PMe_3$)(CO)$_3$ complex (Table 1). As discussed later, the bonding site at Mo($P^iPr_3$)$_2$(CO)$_3$ is amphoteric, and binding of $\sigma$-donors such as quinuclidine should be favorable except for steric repulsions. Binding of ammonia and primary ammines is known for Mo($P^iPr_3$)$_2$(CO)$_3$,[1] however, these ligands were not investigated because of the complexity of H-bonding in these systems. The primary $\sigma$-donor ligands $PPh_2Me$ and P(OMe)$_3$ actually form stronger bonds to W($PCy_3$)(CO)$_3$ than do any of the N donors investigated here.[29f,29g] Pyridine is a stronger $\sigma$ donor and weaker $\pi$ acceptor than are nitriles, but, as shown in the data in Table 4, binds with equal enthalpy as nitriles. The fact that the methyl pyrazine cation binds ≈ 2.5 kcal/mol more strongly than pyrazine is indicative of the greater $\pi$-backbonding ability of the cation. This also shows up clearly in the computed HOMOs for these ligands as shown in Supporting Information, Figure SF-8.

The preferred binding of bridging versus terminal pyrazine (4.4 kcal $mol^{-1}$) as opposed to the preferred binding of $N_2$ as a terminal rather than a bridging ligand ($\approx$ 1.5 kcal $mol^{-1}$) warrants additional comment. The lower stability of the $\mu$-$N_2$ binding architecture may be due to steric factors which should be alleviated in the $\mu$-pyrazine complex. Computation does not estimate the stability of either complex well, but does a somewhat better job on the $Mo(PMe_3)_2(CO)_3$ complexes. The reasons for the disparity between experiment and theory in calculation of the bridging pyrazine stability are not known but may be due to overestimation of steric repulsive terms as discussed earlier. Additional work in this area with other metal complexes is planned and may add additional insight.

**Comparisons to Gas-Phase Proton Affinities.** The gas-phase proton affinity of $N_2$ is 118 kcal $mol^{-1}$ compared to 186 kcal $mol^{-1}$ for $CH_3CN$ and 194 kcal $mol^{-1}$ for $C_6H_5CN$. Taking an average of 190 kcal $mol^{-1}$ for the nitriles, the ratio of PAs is 118/190 = 0.62. In comparing the estimated absolute bond strengths to $Mo(P^iPr_3)_2(CO)_3$ of $\approx$ 17 kcal $mol^{-1}$ for $N_2$ and 24 kcal $mol^{-1}$ for nitriles (see Supporting Information, Table ST-1), it can be seen that the bond strength ratio to the Mo complex is $\approx$ 17/24 = 0.7. The close agreement of these ratios does not allow discounting the role of $\sigma$-donation for $N_2$, and implies that the extent of $\sigma$ donation may be roughly proportional to the relative proton affinity of $N_2$. In addition, it should be noted that binding of $N_2$ results in an increase in the average wavenumber of vibrations of the CO ligands in $Mo(P^iPr_3)_2(CO)_3$. Thus, in a crude sense, $N_2$ could be said to be more electron donating than the agostic bond which it displaces. The largest $N_2$ vibrational shift, $\Delta\nu_{NN} = -178$ $cm^{-1}$, occurs for $N_2$ binding to $Mo(P^iPr_3)_2(CO)_3$. This compares to the largest shift, $\Delta\nu_{NCR}$ of $-68$ $cm^{-1}$, upon coordination by a nitrile for $C_6F_5CN$. As discussed earlier, in backbonding to nitriles the frequency shift of the nitrile may not reflect the total situation with respect to backbonding since a significant contribution is into the $\pi^*$ orbitals of the arene. It seems likely that as a fraction of the net bonding, backbonding plays a larger role in $N_2$ binding than it does in $C_6F_5CN$ binding. Discounting the role of $\sigma$-donation in binding of $N_2$ does not, however, seem warranted for $Mo(P^iPr_3)_2(CO)_3$.

## Conclusions

The interaction between ligands and metals depends on the properties of both. This work investigates that matchup between NX donor/acceptor ligands and acceptor/donor properties of $M(P^iPr_3)_2(CO)_3$, M = Mo,W. The amphoteric nature of the active site at $W(P^iPr_3)_2(CO)_3$ is illustrated by its most famous reaction: it can accommodate dihydrogen as either a molecular hydrogen complex or a dihydride. Earlier work has shown that while $W(PCy_3)_2(CO)_3$ binds CO more strongly than $PMe_2Ph$,[4] the W-$PMe_2Ph$ bond (which relies primarily on the $\sigma$-donor ability of the phosphine) is nevertheless quite strong in spite of the steric repulsion engendered by forming $W(PCy_3)_2(CO)_3(PMe_2Ph)$. The ligands investigated here, dinitrogen, nitriles, azides, diazoalkanes, and so on, are also amphoteric in the sense that both $\sigma$-donor ability and $\pi$-acceptor character play important roles in the binding. A range of $\approx$10 kcal $mol^{-1}$ was found in the enthalpies of ligand binding, and good correlation was found between theory and experiment in terms of structure and spectral parameters for the complexes involved. A reasonable correlation between experimental and computational bond strengths for the NX ligands studied here has been achieved with the exception of bridging dinuclear structures, which require further work beyond the scope of this paper. No simple picture emerges; a blend of factors is involved in the bonding. The planar nature of the dimethyl amino group in bound $Me_2NCN$ as shown in Figure 4 is an indication of $\pi$-bonding effects as is the significantly lowered frequency of the carbonyl ligand in $N_2CHC(=O)OEt$ upon coordination. As discussed for the HOMO and LUMO pictures of nitrile binding shown in Figure 10, it can be difficult to assess spectroscopically how significant $\pi$-back bonding is. The near constant enthalpies of binding of nitrile ligands in spite of a range of spectroscopic and color changes show that even as the nature of the metal−ligand bond is systematically changing, its interaction energy may remain constant. That result was surprising, but seems in accord with what has been previously learned from studies[1] of $H_2$ interactions at the binding site in the complexes $M(CO)_3(PR_3)_2$, M = Cr, Mo, W; R = $^i$Pr, Cy. Investigation of binding of NX ligands to a wider range of metal complexes is in progress to see if the binding trends found here apply to other metal complexes where the $\sigma$ acceptor/$\pi$ donor properties of the metal complex may not be as closely balanced.

**Acknowledgment.** The authors dedicate this paper to Dr. Gregory J. Kubas. Support of this work by the National Science Foundation (Grant CHE 0615743) is gratefully acknowledged (C.D.H.). The work at Brookhaven National Laboratory is funded under contract DE-AC02-98CH10886 with the U.S. Department of Energy and supported by its Division of Chemical Sciences, Geosciences, & Biosciences, Office of Basic Energy Sciences. M.T. thanks the Spanish Ministry of Science and Innovation and the Fulbright commission under Fellowship FU-2006-1738.

**Supporting Information Available:** Supplemental FTIR spectra, computational UV−vis spectra, computational drawings of HOMO and LUMO orbitals of $M(NR)(P^iPr_3)_2(CO)_3$, XRD structures, XRD data tables, and CIF files for all single crystal structure determinations. This material is available free of charge via the Internet at http://pubs.acs.org.